

# Assessment and Estimation of Groundwater Recharge Using SWAT Model in Upper Wabe Shebele River Basin, South-Eastern Ethiopia



Mustefa Aliyi Fejiso

A Thesis Submitted to the Department of Applied Geology

School of Applied Natural Science

Presented in Partial Fulfillment of the Requirement for the Degree of

Master of Science in Applied Geology

Office of Graduate Studies

Adama Science and Technology University

December, 2024

Adama, Ethiopia

Assessment and Estimation of Groundwater Recharge Using SWAT Model in  
Upper Wabe Shebele River Basin, South-Eastern Ethiopia

Mustefa Aliyi Fejiso

Major Advisor:

Muhammed Haji (PhD)

Co-Advisor:

Hassen Shube (PhD)

A Thesis Submitted to the Department of Applied Geology

School of Applied Natural Science

Presented in Partial Fulfillment of the Requirement for the Degree of

Master of Science in Applied Geology

Office of Graduate Studies

Adama Science and Technology University

December, 2024

Adama, Ethiopia

## DECLARATION

I hereby declare that this Master Thesis entitled “Assessment and Estimation of Groundwater Recharge Using SWAT Model in Upper Wabe Shebele River Basin, South-Eastern Ethiopia” is my original work. That is, it has not been submitted for the award of any academic degree, diploma, or certificate in any other university. All sources of materials used for this thesis have been duly acknowledged through the citation.

Mustefa Aliyi Fejiso

---

Name of the Student:

Signature

Date

## RECOMMENDATION

We, the advisors of this thesis, hereby certify that we have read the revised version of the thesis entitled “**Assessment and Estimation of Groundwater Recharge Using SWAT Model in Upper Wabe Shebele River Basin, South-Eastern Ethiopia**” prepared under our guidance by Mustefa Aliyi Fejiso submitted in partial fulfillment of the requirements for the degree of Master of Science in Applied Geology. Therefore, we recommend the submission of revised version of the thesis to the department following the applicable procedures.

---

Major Advisor:

Signature

Date

---

Co-advisor:

Signature

Date

## APPROVAL PAGE OF THESIS

We, the advisors of the thesis entitled “**Assessment and Estimation of Groundwater Recharge Using SWAT Model in Upper Wabe Shebele River Basin, South-Eastern Ethiopia**” and developed by Mustefa Aliyi Fejiso, hereby certify that the recommendation and suggestions made by the board of examiners are appropriately incorporated into the final version of the thesis.

---

Major Advisor:	Signature	Date
----------------	-----------	------

---

Co-advisor:	Signature	Date
-------------	-----------	------

We, the undersigned, members of the Board of Examiners of the thesis by Mustefa Aliyi Fejiso have read and evaluated his thesis entitled “Assessment and Estimation of Groundwater Recharge Using SWAT Model in Upper Wabe Shebele River Basin, South-Eastern Ethiopia” and examined the candidate during open defense. This is, therefore, to certify that the thesis has been accepted in partial fulfillment of the requirement of the Degree of Master of Science applied Geology.

---

Chairperson:	Signature	Date
--------------	-----------	------

---

Internal Examiner:	Signature	Date
--------------------	-----------	------

---

External Examiner:	Signature	Date
--------------------	-----------	------

Finally, approval and acceptance of the thesis is contingent upon submission of its final copy to the Office of Postgraduate Studies (OPGS) through the Department Graduate Council (DGC) and School Graduate Committee (SGC).

---

Department Head:	Signature	Date
------------------	-----------	------

---

School Dean:	Signature	Date
--------------	-----------	------

---

Office of Postgraduate Studies, Dean:	Signature	Date
---------------------------------------	-----------	------

## **ACKNOWLEDGEMENT**

First and foremost, I wish to express my heartfelt gratitude to Allah, my guiding mentor and unwavering support throughout both my personal and academic journeys. I am deeply appreciative of my beloved family, especially my mother, Kedija Beriso, and my father, Aliyi Fejiso. Their steadfast love, prayers, and selfless acts have continually inspired and supported me in all aspects of my life and education.

I humbly extend my heartfelt appreciation to my thesis Advisor's, Dr. Muhammad Haji and Dr. Hassen Shube, for their continuous guidance, motivation, and assistance. Their expertise, understanding, and dedication to my progress have been invaluable, motivating me to pursue excellence in this research project. I extend my heartfelt appreciation to Adama Science and Technology University, and all staff of Applied Geology Department. I also wish to extend my truthful gratitude to my friends and all individuals who have contributed to the successful completion of this study.

# TABLE OF CONTENTS

<b>Contents</b>	<b>Pages</b>
<b>ACKNOWLEDGEMENT .....</b>	<b>i</b>
<b>TABLE OF CONTENTS .....</b>	<b>ii</b>
<b>LIST OF TABLES.....</b>	<b>vi</b>
<b>LIST OF FIGURES .....</b>	<b>vii</b>
<b>LIST OF ACRONYMS AND ABBREVIATIONS .....</b>	<b>ix</b>
<b>ABSTRACT .....</b>	<b>x</b>
<b>CHAPTER ONE .....</b>	<b>1</b>
<b>1. INTRODUCTION.....</b>	<b>1</b>
1.1 Background of the Study .....	1
1.2 Statement of the Problem.....	5
1.3 Research Question .....	6
1.4 Objective.....	6
1.4.1 General Objective.....	6
1.4.2 Specific Objectives.....	6
1.5 Significance of the Study .....	7
<b>CHAPTER TWO .....</b>	<b>8</b>
<b>2. LITERATURE REVIEW.....</b>	<b>8</b>
2.1 Groundwater Recharge .....	8
2.2 Groundwater recharge estimation.....	10
2.3 Groundwater Recharge Models .....	12

2.3.1 General .....	12
2.3.2 SWAT Model concepts .....	13
<b>CHAPTER THREE .....</b>	<b>18</b>
<b>3. DESCRIPTION OF THE STUDY AREA .....</b>	<b>18</b>
3.1 Location and accessibility.....	18
3.2 Climatic Condition.....	19
3.3 Drainage.....	20
3.4 Physiography .....	21
3.5 Regional Geology .....	22
3.6 Local geology .....	24
3.6.1 Nazreth Group and Dino Formation.....	24
3.6.2 The plateau basalt.....	24
3.6.3 The upper pyroclasts .....	24
3.6.4 The highland basalt flows .....	25
3.6.5 Alkali trachyte flows with some plugs .....	25
3.6.6 Trachytic tuffs with minor basalt and alkali trachyte flows and sediments .....	25
3.6.7 Interlayered alkali trachyte and basalt flows.....	25
3.6.8 Pliocene basalt flows.....	26
3.6.9 Pliocene trachyte flows .....	26
3.6.10 Quaternary alluvial deposits.....	26
3.7 Geological Structure .....	27
3.8 Hydrogeology .....	29
3.8.1 General .....	29
3.8.2 Extensive and High Productive Fracture and/or Porous Volcanic Aquifer .....	29

3.8.3 Extensively developed medium to high productive, fractured, jointed and porous aquifer.....	30
3.8.4 Extensive and Moderately Productive Fissured Aquifers .....	31
3.8.5 Extensively developed low to medium productive fractured aquifer .....	31
3.8.6 Extensive and Low Productive Fractured Volcanic Aquifer .....	31
3.9 Ground Water Flow, Recharge and Discharge .....	33
<b>CHAPTER FOUR.....</b>	<b>35</b>
<b>4. METHODS AND MATERIALS .....</b>	<b>35</b>
4.1 Desk study.....	35
4.2 Data Collection .....	35
4.3 SWAT Input Data Preparation and their Sources .....	35
4.3.1 Digital Elevation Models (DEM).....	36
4.3.2 Land-Use/Land Cover (LULC).....	36
4.3.3 Soil data.....	37
4.3.4 Slope.....	39
4.3.5 Climate data.....	40
4.3.6 Stream flow data.....	41
4.4 SWAT Model set up .....	41
4.4.1 Watershed Delineation .....	41
4.4.2 Hydrologic Response Units.....	42
4.4.3 Weather data definition .....	43
4.5 Model uncertainty analysis .....	43
4.6 Model Sensitivity analysis .....	44
4.7 Model calibration and validation .....	47
4.8 Materials Used .....	49

<b>CHAPTER FIVE .....</b>	<b>51</b>
<b>5. RESULT AND DISCUSSION .....</b>	<b>51</b>
5.1 Annual water balance .....	51
5.2 Spatial distribution of Precipitation, Surface runoff, and Evapotranspiration .....	52
5.3 Groundwater Recharge .....	56
5.3.1 Spatial groundwater recharge variability .....	56
5.3.2 Temporal groundwater recharge variability .....	59
5.4 Governing factors for variability of groundwater recharge .....	66
5.5 Model performance evaluation .....	69
<b>CHAPTER SIX .....</b>	<b>72</b>
<b>6. CONCLUSIONS AND RECOMMENDATIONS .....</b>	<b>72</b>
6.1 Conclusion .....	72
6.2 Recommendation .....	74
<b>REFERENCES .....</b>	<b>75</b>
<b>APPENDIXES.....</b>	<b>i</b>

## LIST OF TABLES

<b>Tables</b>	<b>Pages</b>
Table 4.1 Distribution LULC type in the Upper Wabe Shebele River Basin.....	37
Table 4.2 Distribution of soil type in the Upper Wabe Shebele River Basin .....	38
Table 4.3 Sensitive flow parameters and their Calibrated range, and Calibrated Value for the SWAT model's simulations of Furuna, Leliso, and Wabe river. ....	46
Table 4.4 Different software's used and their purpose .....	49
Table 5.1 Annual water balance of the Upper Wabe Shebelle Basin (UWSB).....	51
Table 5.2 Goodness fit considered for model .....	70

# LIST OF FIGURES

<b>Figures</b>	<b>Pages</b>
Figure 2.1 Schematic representation of the hydrologic cycle in SWAT model (Neitch et al., 2005).....	14
Figure 3.1 Location map of the study area.....	19
Figure 3.2 Average monthly climate distribution across six stations (Adaba, Ardayita, Dodola, Hunte, Kofale, and Meraro) in the study area. ....	20
Figure 3.3 Drainage map of study area .....	21
Figure 3.4 Physiographic map of study area .....	22
Figure 3.5 Geological map of Upper Wabe Shebele river basin and distribution of the lineaments in the region (adapted from (Alemayehu et al., 1991; Aman et al., 2012; Basalfew et al., 2012; Workineh et al., 2013)). .....	28
Figure 3.6 Hydrogeological map of Upper Wabe Shebele basin (adapted from (Agezew et al., 2014; Astatike Kiflu & H/Mariam, 2010; Astatke et al., 2009; Kiflu, 2010; Tilahun & Sima, 2013)). .....	32
Figure 4.1 LULC map of Upper Wabe Shebele River Basin.....	37
Figure 4. 2 Soil Map of Upper Wabe Shebele Basin.....	38
Figure 4.3 Slope map of Upper Wabe Shebele River basin .....	39
Figure 4.4 Sensitivity analysis using SWAT-CUP based on t-stat and p-value .....	45
Figure 4.5 Flowchart of the Research Methodology. ....	50
Figure 5.1 The average water balance components for the entire simulation period (2000-2018) of the Upper Wabe Shebele river basin.....	52
Figure 5.2 The long term (2000-2018) annual spatial distribution of water balance components: A) Precipitation, B) Surface Runoff. and C) Evapotranspiration.....	56
Figure 5.3 Spatial groundwater recharge map of the Upper Wabe Shebele Basin.....	59
Figure 5.4 Spatial variability of groundwater recharge within year from season to season. (A) October-January (Bega season), (B) February-May (Belg season) and (C) June-September (Kiremt). .....	61

Figure 5.5 Average monthly groundwater recharge with compared to average monthly precipitation at different physiographic regions (mm/month) within the study area. A) WPLT, CPLT, SHL, and NHL Average monthly precipitations (mm/month), and B) WPLT, CPLT, SHL and NHL groundwater recharge (mm/year)..... 63

Figure 5.6 Average annual groundwater recharge with compared to average annual precipitation at different physiographic regions. A) WPLT, CPLT, SHL, NHL precipitation (mm/year), B) WPLT, CPLT, SHL, NHL groundwater recharge (mm/year). ..... 65

Figure 5.7 Average annual variation in climate (precipitation and temperature) across various physiographic regions of Upper Wabe Shebele river basin..... 67

Figure 5.8 Monthly time series of measured and simulated average discharge of A) Furuna B) Leliso and C) Wabe River for the calibration (2000-2011) and validation (2012-2018) periods. .... 71

## LIST OF ACRONYMS AND ABBREVIATIONS

ASTU	Adama Science and Technology University
CPLT	Central Plateau
DEM	Digital Elevation Model
ECO	Engineering Corporation of Oromia
FAO	Food and Agriculture Organization
HRU	Hydrologic Response Unit
ITCZ	Inter Tropical Convergence Zone
LULC	Land-Use/Land Cover
NHL	Northern Highland
NSE	Nash-Sutcliffe efficiency
PBIAS	Percent Bias
R <sup>2</sup>	Coefficient of Determination
SHL	Southern Highland
SWAT	Soil and Water Assessment Tool
SWAT-CUP	Soil and Water Assessment Tool-Calibration and Uncertainty Programming
SUFI-2	Sequential Uncertainty Fitting Version 2
USGS	US Geological Survey
UWSB	Upper Wabe Shebelle Basin
WPLT	Western Plateau

## ABSTRACT

*In Upper Wabe Shebelle River Basin, groundwater is a key resource that supplements surface water to meet the demands of humans and the ecosystem. Therefore, it is essential to quantify groundwater recharge rate which is crucial for water resource development and management. This study utilized the SWAT (Soil and Water Assessment Tool) model to quantify the groundwater recharge rate and its spatial distribution in the Upper Wabe Shebele river basin of southeastern Ethiopia, aiming for improved groundwater resource planning and management. Hydro-meteorological data from, 2000 to 2018 was utilized for SWAT model calibration, and validation purposes. The performance evaluation showed acceptable ranges of model evaluation indicators ( $R^2 = 0.65-0.88$ ,  $NSE = 0.58-0.77$ ,  $PBIAS = 5.13-14.0$ ). The spatial average annual groundwater recharge decreases from the highlands (315 mm/year) to the central plains (101 mm/year), with both seasonal and annual variations closely mirroring precipitation patterns throughout the catchment. The simulated water budget of the entire watershed revealed that approximately 214.60mm of the mean annual precipitation that occurs in the watershed was attributed to groundwater recharge. This quantity represents approximately 22.33% of the mean annual precipitation in the watershed. Ultimately, the variability of groundwater recharge is primarily driven by changes in precipitation. The remaining precipitation is partitioned into evapotranspiration (549.55mm), surface runoff (180.10mm) and (14.75mm) allocated to baseflow. The long-term annual water balance from 2000 to 2018 indicated that evapotranspiration is the most dominant factor accounting for approximately 57.19% of the mean annual precipitation in the catchment. In generally, findings of this study reveal that groundwater recharge in the Upper Wabe Shebelle River Basin exhibits significant seasonal and annual variability, and these variations were principally driven by fluctuations in precipitation. By utilizing the SWAT model, it provides valuable insights that can inform sustainable water management practices in the catchment area.*

**Keywords:** GWR, UWSRB, SWAT model, Southeastern Ethiopia,

# CHAPTER ONE

## 1. INTRODUCTION

### 1.1 Background of the Study

Groundwater is the major source of fresh water and the best alternative to the surface-water supply required for agricultural, domestic and industrial purposes. Throughout the globe, groundwater holds immense significance as a vital and indispensable source of fresh water (Healy, 2017). It serves as a lifeline for numerous communities and industries, providing a reliable and sustainable water supply. It is considered a valuable and stable freshwater asset that plays a vital role in human well-being and regional development, particularly in areas with limited freshwater sources (Dehghan et al., 2024). Groundwater is globally recognized for its reliability and higher quality, as it is protected from surface pollution and less susceptible to immediate contamination. In Africa alone, it serves as a dependable water source for over 100 million people and has the potential to assist millions more, particularly in rural areas with high demand. Similarly, groundwater is the main source for drinking water supply in many parts of Ethiopia that cover more than 70% of Ethiopia's water supply and only 34% of the population has access to an improved water supply (IAEA, 2013). In addition, the groundwater of the Ethiopian volcanic aquifer sustains the existence of wetlands and lakes including their ecosystems (Billi, 2015). In order to utilize this precious resource for sustainable development, understanding of groundwater potential, particularly the recharge and its evaluation is essential.

Groundwater recharge occurs when rainfall water infiltrates the saturated zone by means of both direct and indirect mechanisms, including through fractures, joints, shrinkage cracks, and sinkholes. It is essential for replenishing aquifers, supporting ecosystems, agriculture, and human societies. However, rainfall distribution may not represent the groundwater recharge distribution as recharge is affected by different factors including soil type, geology, slope, and land cover. For instance, when it comes to influencing groundwater resources, modifications in Land Use and Land Cover (LULC) are prominent anthropogenic catalysts, primarily due to their impact on groundwater recharge (Han et al., 2017). Especially in a region with a complex topographic nature such as Ethiopian watersheds considering rainfall distribution as the main

factor in the groundwater potential mapping may result in misleading conclusions. In a data-scarce region, understanding the spatiotemporal distribution of the recharge adds significant value to the sustainable management of the resource.

The Upper Wabe Shebelle River basin is located in Southeastern Ethiopian plateau that characterized by a thick monotonous, rapidly erupted pile of locally deformed, flat lying basalts consisting of a number of volcanic centers with different magmatic character and with a large range of ages (Mohr, P.A. and Potter, 1976; Mohr and Zanettin, 1983). The variety of landforms of the basin is of significant importance to groundwater occurrence and movement where the interlayer of acidic lava and ash components with fractured basaltic layers create a unique feature for groundwater storage in movement. Apart from the significance of these prominent geomorphic characteristics in the groundwater recharge and circulation, the structure of the lava flow units makes the shield volcanoes a distinct hydrogeologic units as compared to the underlying horizontally lain flood basalt plateau (Kebede, 2013). Despite the vital role that groundwater plays in most people's lives, little detailed hydrogeological studies have been conducted in the volcanic rocks of Ethiopia, particularly in the South Eastern Ethiopian Plateau. There is a surface water resource in the Upper Wabe Shebele basin that the community uses for different domestic and agricultural activities. But there are only scarce or no information on the amount of groundwater recharge for wise and sustainable utilization and proper management of the limited water resources. Thus, the estimation of groundwater recharge in the basin plays its own role in solving the problems related to the management and planning of water resources for sustainable development using hydrological models with the help of GIS and RS techniques.

Estimates of rates of groundwater recharge are of prime importance in the assessment, development, and utilization of groundwater resources, on the one hand, and their protection against pollution and depletion, on the other (Gaye and Edmunds, 1996). There have been various methods developed to quantify the amount of groundwater recharge. These include point measurement using lysimeters (Grasso et al., 2003) which involves direct measurements at specific locations. Another approach is the water balance method applied at the basin level (Mjemah et al., 2011), which considers the overall water inputs and outputs in a given area. The water table fluctuation method (Gerhat, 1986) examines changes in the groundwater table to estimate recharge. Additionally, the Darcy method is utilized to assess groundwater flow and

recharge. However, it is important to note that existing techniques for quantifying groundwater recharge lack certainty in accounting for the spatiotemporal variability of factors such as rainfall patterns, soil and geological properties, and land use changes that influence recharge. Therefore, there is a need for more robust and comprehensive approaches that can capture the complex dynamics of groundwater recharge accurately. Due to a scarcity of comprehensive data on crucial aspects such as aquifer properties and observed groundwater dynamics at a large scale, it appears that experimental approaches may not be the most suitable course of action. The limited availability of such information hampers the ability to design and execute effective experiments that can accurately represent real-world conditions. Consequently, alternative methodologies or approaches that rely on existing data or modeling techniques might be more appropriate in this context. The main goal of this study is to characterize the spatial and temporal variability of recharge and identify the various drivers that govern its distribution. To account for the spatial heterogeneity of the basin in terms of soil, land-use and slope characteristics, the semi-distributed hydrologic model SWAT (Arnold et al., 1998; Neitsch et al., 2011) is employed. In addition, the model-based estimation of groundwater recharge allows examining the sensitivity of groundwater recharge to changes in air temperature and precipitation. This represents a first step towards an assessment of the aquifers' vulnerability to climate change.

Hydrological models have become essential instruments for understanding hydrologic processes on a watershed level, and their widespread use for hydrologic prediction (Beven, 2006; Gassman et al., 2007). The development and advancement of hydrological models have transformed them into indispensable tools for understanding hydrologic processes at the watershed scale. These models are broadly utilized for predicting hydrologic events and phenomena. The SWAT (Soil and Water Assessment Tool) model, is a distributed, continuous, and long-term watershed-scale model specifically designed to forecast the effects of land management practices on hydrology, sediment, and contaminant transport within agricultural watersheds (Setegn et al., 2010). SWAT model operates at the basin scale using a daily time step, efficiently simulating continuous processes over long periods (Kim et al., 2008). The watershed is divided into sub-watersheds, further subdivided into homogeneous hydrologic response units (HRUs) based on land use and management.

Within this research attempt, the simulation of groundwater recharge is undertaken within a watershed predominantly characterized by humid climate, covering an extensive area of 4413 km<sup>2</sup>. This is achieved through the integration of meteorological data, soil data, LULC data, and slope into the SWAT model, enabling the quantification of groundwater recharge. The approach employed in this study involves assessing the parameter that affect groundwater recharge during calibration periods by using stream flow data. This study carefully considered the available observed hydro-meteorological data for the Upper Wabe Shebele River Basin to address potential sources of uncertainty in the model simulation. The main objective of this study was to assess and quantify the groundwater recharge rates in the Upper Wabe Shebele Basin using the SWAT model for better planning and management of groundwater resource.

## **1.2 Statement of the Problem**

The current understanding of groundwater recharge rates in extensive regions of Ethiopia remains limited, posing challenges for accurate estimation. However, accurate estimation of groundwater recharge is increasingly necessary due to its significant role in various hydrological assessments. This is especially crucial for sustainable water resource management. In Upper Wabe Shebelle River Basin, groundwater is a key resource that supplements surface water to meet the demands of humans and the ecosystem. Although groundwater plays a vital role in daily life, there is a lack of comprehensive hydrogeological studies on the volcanic rocks of Ethiopia, particularly in the Southeastern Ethiopian Plateau. The local community depends on surface water from the Upper Wabe Shebele River basin for domestic and agricultural purposes. But there are only scarce or no information on the amount of groundwater recharge for wise and sustainable utilization and proper management of the limited water resources.

The absence of comprehensive understanding and reliable estimation for groundwater recharge studies in this region hinders effective management and sustainable utilization of water resources. Furthermore, the impacts of climate change and land use changes are intensifying, creating an urgent need to comprehend the spatial and temporal patterns of groundwater recharge. Moreover, there is intense agricultural activities in the basin where mainly wheat is produced based on rainfall. However, the government is shifting to produce the wheat using irrigation system in addition to rain-based agriculture. The available surface water in the basin is not enough for winter irrigation and the supplement of groundwater is a needed. Hence, it is essential to quantify the spatial and temporal rate of replenishment of the aquifers in the region for sustainable water resource development and management. Addressing these areas of limited knowledge requires focused research efforts aimed at quantifying groundwater recharge rates in the Upper Wabe Shebele River Basin by utilizing SWAT modeling approaches. The information obtained from this work will enable policymakers and water resource managers to make informed decisions regarding the allocation and conservation of groundwater resources in the region.

## 1.3 Research Question

This research work is expected to answer the following research questions:

- ✚ What is the groundwater recharge rates in the Upper Wabe Shebele Basin and what insights can be gained from these estimations to support sustainable water resource management in the study area?
- ✚ What are the spatial and temporal patterns of groundwater recharge in the Upper Wabe Shebele Basin?
- ✚ Furthermore, what are the limitations and uncertainties associated with the application of SWAT modeling in estimating groundwater recharge in this specific basin?

## 1.4 Objective

### 1.4.1 General Objective

To assess and quantify the groundwater recharge rates in the Upper Wabe Shebele River Basin using the SWAT model for better planning and management of groundwater resource.

### 1.4.2 Specific Objectives

- ✚ To delineate hydrologic response units for the catchment.
- ✚ To determine spatial and temporal patterns of groundwater recharge of the catchment
- ✚ To estimate distributed seasonal and annual groundwater recharge of the catchment.
- ✚ To estimate distributed annual actual evapotranspiration and surface runoff of the catchment.
- ✚ To identify the main driving factors that govern the distribution of groundwater recharge.

## 1.5 Significance of the Study

- ✚ The research aims to enhance understanding of groundwater recharge processes in the Upper Wabe Shebele Basin. By estimating recharge rates, it will provide valuable insights into the availability and sustainability of groundwater resources in the region.
- ✚ Accurate estimation of groundwater recharge is crucial for effective water resource management. The findings from this study will help policymakers, water managers, and stakeholders to make informed decisions regarding the allocation and utilization of groundwater resources in the study area.
- ✚ The research findings will add to the existing body of scientific knowledge on groundwater recharge estimation. By focusing on the Upper Wabe Shebele Basin, the study will provide specific insights into groundwater recharge processes in this region, which can contribute to the broader understanding of hydrological processes in similar climatic and geological settings.

## CHAPTER TWO

### 2. LITERATURE REVIEW

#### 2.1 Groundwater Recharge

Groundwater recharge is the movement of water from source such as: precipitation, canals, rivers, lakes, and streams as it percolates through the soil and enters to the aquifers (Caritat, 1997). It is defined as the portion of rainfall that reaches the saturated zone, either through direct contact in the riparian zone or downward percolation in the unsaturated zone. It can also occur as a result of human activities and interventions (Jeffrey et al., 1993). Numerous factors, including precipitation properties, vegetation cover, topography, soil composition, and geological characteristics are influence the extent of water infiltration into the water table (Adams et al., 2004).The quantity of groundwater present in the subsurface depends on the porous nature of rocks and their spatial distribution. Variations in groundwater potential across different regions, countries, and continents are closely connected to factors such as the type and extent of rocks, as well as the rates and conditions of recharge.

Several factors affect the groundwater recharge rate and climate variability plays a fundamental role in determining the variation of recharge rates. Changes in temperature, precipitation, and evapotranspiration directly affect the availability and movement of water within the hydrological cycle, eventually impacting groundwater recharge processes. The primary driver of natural recharge, precipitation, arises as the dominant factor within the water budget of most watersheds (Jannis et al., 2021). Rising temperatures associated with climate change can lead to increased evaporation rates, which can reduce the amount of water available for groundwater recharge (Bridget et al., 2002). Higher temperatures can also increase plant transpiration, further exhausting soil moisture and reducing recharge. The topography of the land surface plays a central role in both diffuse and focused recharge processes. It influences the way water interacts with the landscape and affects the rates of infiltration and runoff. Steep slopes, characterized by their significant incline, tend to have low infiltration rates and high runoff rates. Infiltration is a crucial process in both natural ecosystems and human activities. It is defined as the

movement of water through the soil surface, entering the soil profile through pores(Andy & Stanley, 2003). This can result in reduced recharge opportunities. On the other hand, flat land surfaces with poor surface drainage provide favorable conditions recharge. The absence of pronounced slopes allows water to spread out more evenly across the surface, increasing the chances of infiltration(Healy, 2017). Permeability of surface and subsurface geologic materials significantly affect recharge. Coarse-grained, high-permeability soils or geologic materials promote recharge by allowing rapid water transmission, while fine-grained, low-permeability soils hinder transmission (Healy, 2017). High-permeability streambeds facilitate surface water and groundwater exchange in focused recharge (Bridget et al., 2002) Both discharge processes and recharge processes, are influenced by subsurface geology. When the rate of discharge from an aquifer is smaller than the infiltration rate, the storage of water within the aquifer increases. At a certain point, aquifer storage can reach its maximum capacity, preventing further acceptance of recharge, even if there is extra precipitation. This situation often results in enlarged runoff.

Surface and subsurface water interconnection is another factor that control groundwater recharge. The depth of the water table plays significant role in groundwater recharge processes. When the unsaturated zone is shallow, water can quickly reach the water table through infiltration, leading to intermittent recharge that occurs mainly in response to significant precipitation events. However, shallow water tables are also susceptible to groundwater discharge through plant transpiration. As a result, water that recharges shallow subsurface systems may only remain in the saturated zone for a short period before being extracted by plant roots and released back into the atmosphere(Healy, 2017). The presence of vegetation and the way land is used can significantly impact the process of recharge. Land use change typically brings about important alterations in flood peak characteristics and infiltration properties, thereby impacting the entire hydrological environment of the area. Assessing the adverse effects resulting from land-use changes necessitates the estimation of changes in surface runoff and groundwater recharge rates(Jinno et al., 2009). The process of urbanization familiarizes various alterations to the land surface, which can have substantial consequences for recharge processes.

## 2.2 Groundwater recharge estimation

The estimation of groundwater recharge is very challenging due to the absence of direct measurement methods commonly used for surface water resources (Bakker et al., 2013). Its occurrence below the Earth's surface, making it inaccessible for direct observation. This complexity arises from water infiltrating through different pathways, such as soil, fractures, and porous rock formations, before replenishing aquifers. Methods for estimating recharge can be divided into different types based on the three hydrologic zones from which the data are derived: surface water, unsaturated zone and saturated zone (Bridget et al., 2002). This subdivision allows for a systematic approach to assess and quantify recharge processes in each particular hydrologic zone. Different methods exist for measuring groundwater recharge, given the diversity of sources and recharge processes. However, each method comes with its limitations regarding reliability and applicability. It's crucial to understand the specific objective of the recharge study before choosing the appropriate method for quantifying groundwater recharge, as this can influence the necessary spatial and temporal scales for the recharge estimates. Procedures used to quantify recharge from the various sources can be generally classified as physical technique, tracer techniques, and numerical modelling approaches. many researchers quantified (qualitatively and quantitatively) recharge rates different techniques.

For instance, (Demlie, 2015) used physical and tracer method conjunctively to quantify groundwater recharge. Watershed (rainfall/runoff) modeling is used to estimate recharge rates over large areas. One of the largely used model is SWAT model that operates at the basin scale and utilizes a continuous time step, typically on a daily basis. In SWAT, a watershed is divided into multiple sub-watersheds, which are further subdivided into hydrologic response units (HRUs). These HRUs represent homogeneous areas within the watershed characterized by similar land use, management practices, and soil properties. It is important to note that the HRUs are not explicitly identified spatially within the SWAT simulation but rather represent proportions of the sub-watershed area. The popularity of the model can be attributed to its ability to integrate intricate temporal and spatial factors, resulting in valuable outputs at both local and regional scales. This capability to consider detailed temporal and spatial effects contributes to the model's wide acceptance and usefulness (Larbi et al., 2020). Estimating groundwater recharge in both unconfined (shallow) and confined (deep) aquifers is a significant outcome of SWAT modeling (Arnold et al., 1993).

The research conducted by (Awan & Ismaeel, 2014) in the Lower Bari Doab Canal (LBDC) command area in Pakistan, which represents a typical irrigated region in a semi-arid climate indicate that the newly proposed technique offers a more comprehensive and precise estimation of groundwater recharge in irrigated areas, especially considering the effects of changing climatic conditions. Wu & Johnston, (2007) conducted a study using the Soil and Water Assessment Tool (SWAT) model to assess its performance in simulating hydrologic response to climatic variability in a Great Lakes Watershed. The research focused specifically on the Pere Marquette River Watershed in Michigan, USA, comparing two contrasting climatic periods. The SWAT model was employed to simulate streamflow and water balance components, with calibration and validation performed using observed streamflow data. Evaluation of the model's performance utilized statistical metrics like Nash-Sutcliffe efficiency (NSE) and coefficient of determination ( $R^2$ ). The findings indicated that the SWAT model effectively simulated hydrologic response to climatic variability in the Pere Marquette River Watershed. However, it was observed that the model's calibration varied between drought and average climatic conditions, suggesting the importance of separate calibration for different climate scenarios. The study also highlighted the significance of incorporating local data and knowledge during model calibration and validation, considering the variation in data availability and quality across different regions. In summary, the study demonstrated that hydrologic models such as SWAT have great potential for managing and planning watersheds. However, it also emphasized the importance of carefully calibrating and validating these models to ensure accurate and reliable results.

Another study in Greece uses the Soil and Water Assessment Tool (SWAT) to assess future groundwater recharge in various catchments, offering insights for developing strategies to address depletion (Busico et al., 2021). The findings revealed that the SWAT model accurately simulated groundwater recharge in both coastal and inland catchments. Furthermore, the study estimated that the inland basin had a higher percentage of recharge compared to runoff, while the coastal basin had a higher percentage of runoff.

## 2.3 Groundwater Recharge Models

### 2.3.1 General

A hydrologic model serves as a simplified representation of several components of a real-world system, such as surface water, soil water, wetlands, groundwater, and etc. Simulation models are commonly used in hydrologic studies to estimate recharge. They offer valuable insights into the functioning of hydrologic systems by identifying factors that impact recharge. These models can predict how changes in climate, water use, land use, and other factors might affect recharge rates. Most hydrological simulation models, such as watershed and groundwater-flow models, rely on water-budget equations. hydrologic model purpose is to simplify comprehension, prediction, and management of water resources. Creating a conceptual model of recharge processes is a crucial in any study focused on understanding recharge mechanisms (Healy, 2017). By identifying the factors that affect recharge, models play significant role in gaining valuable perceptions into the functioning of hydrologic systems. These models possess predictive capabilities that enable the assessment of how different factors, such as climate change, water utilization, land use modifications, and other might influence recharge rates(Healy, 2017). Groundwater recharge processes show variability across different locations, and it cannot be confident that a methodology developed and employed in one area will produce dependable outcomes when applied in another place. Hydrological models can be categorized based on input and parameters employed, as well as the level of physical principles incorporated within the model. Based on the spatial variability of model parameters, they can be classified as lumped, semi-distributed, or distributed models (Cunderlik, 2003)

Lumped models focus merely on the basin response at the outlet and do not consider spatial variability. These models are generally not appropriate for event-scale processes. However, if the primary interest is in discharge prediction and complex physically-based models are not necessary, lumped models can still provide reliable simulations (Cunderlik, 2003). Distributed models permit the spatial variation of parameters, consenting them to vary at a resolution determined by the user. This modeling method aims to incorporate information on the spatial distribution of parameter dissimilarities and employs computational algorithms to assess the impact of this distribution on simulated precipitation-runoff behavior. Distributed models

typically necessitate a substantial amount of data, which may not always be readily available. However, they offer a detailed representation of the governing physical processes and, when properly executed, can provide the highest level of accuracy (Cunderlik, 2003). Semi-distributed models permit partial spatial discrepancy of parameters by dividing the basin into multiple sub-basins. These models are structured based on the principles of lumped models but offer more spatial resolution. Compared to fully distributed models, they are less dependent on extensive input data requirements.

### 2.3.2 SWAT Model concepts

The hydrological simulations of a watershed in SWAT are divided into two primary phases: the land phase and the routing phase. The land phase focuses on regulating the quantities of water, sediment, nutrients, and pesticides flowing into the main channel of each subbasin within the watershed. On the other hand, the routing phase examines the movement of water, sediment, and agricultural chemicals as they traverse the channel network towards the outlet of the watershed. To model the land phase of the hydrologic cycle, SWAT utilizes the water balance equation (Neitch et al., 2005). Water balance serves as the essential factor governing all processes within SWAT, as it influences various components of the hydrological cycle. These components include surface runoff, vertical movement of water in the soil profile (both downward and upward), horizontal water movement, and the overall water yield (Nasiri et al., 2020). The water balance is calculated using the following equation.

$$SW_t = SW_o + \sum_{i=0}^t (R_{day} - Q_{surf} - Ea - W_{seep} - Q_{gw}) \dots \dots \dots (1)$$

In the equation,  $SW_t$  represents the final soil water content in millimeters (mm),  $SW_o$  represents the initial soil water content on day  $i$  in mm,  $t$  denotes the time in days,  $R_{day}$  represents the amount of precipitation on day  $i$  in mm,  $Q_{surf}$  represents the amount of surface runoff on day  $i$  in mm,  $Ea$  represents the amount of evapotranspiration on day  $i$  in mm,  $W_{seep}$  represents the amount of water entering the vadose zone from the soil profile on day  $i$  in mm, and  $Q_{gw}$  represents the amount of return flow on day  $i$  in mm.

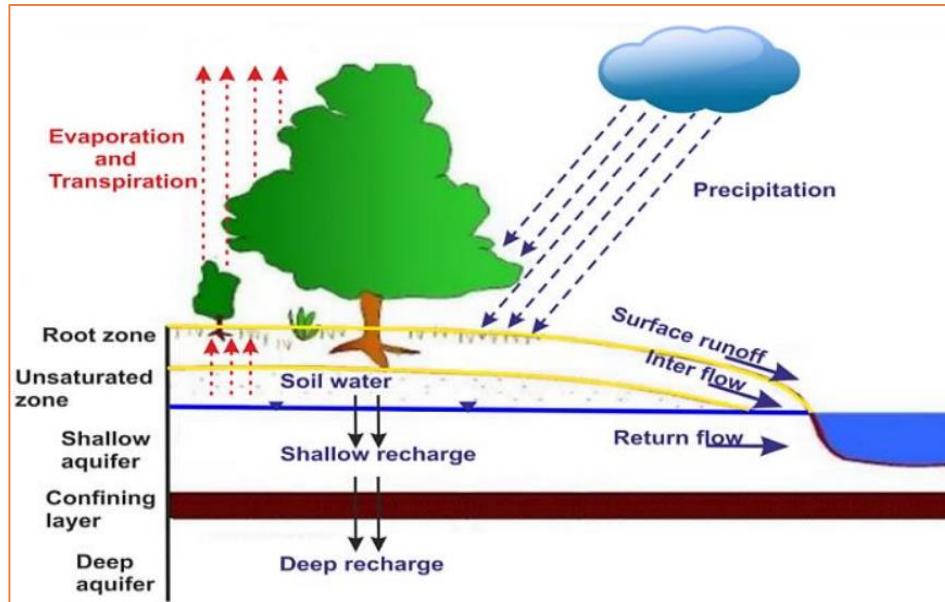


Figure 2.1 Schematic representation of the hydrologic cycle in SWAT model (Neitch et al., 2005)

Within SWAT, the majority of hydrologic processes occur at the Hydrologic Response Unit (HRU) level. At this level, the water balance components are simulated, and later these simulations are aggregated to the sub-basin and basin scales. The key hydrologic components modeled in SWAT, as represented in the water balance equation, include precipitation, surface runoff, evapotranspiration, and groundwater recharge (Moriassi et al., 2012).

### A. Precipitation

Precipitation plays a crucial role in regulating the water balance within a basin as it serves as the primary mechanism through which water enters the land phase of the hydrologic cycle (Moriassi et al., 2012). In the context of SWAT, precipitation is considered one of the fundamental and essential input data types necessary for accurately modeling the hydrology of a basin. Precipitation data can be acquired from observed records or generated by SWAT during the simulation process. According to (Guzman et al., 2015), it is strongly advised to incorporate observed precipitation data whenever it is accessible. The incorporation of observed precipitation data significantly enhances SWAT's ability to replicate observed stream hydrographs, thus improving the model's overall performance and accuracy. By incorporating

observed precipitation data into the SWAT model, the simulated hydrological processes become more representative of the actual conditions experienced in the basin. This enables a more reliable assessment of the water balance components and enhances the model's ability to capture the dynamics of the hydrologic system.

**B. Surface Runoff**

Surface runoff takes place when the rate of water precipitation surpasses the soil's infiltration capacity, leading to the saturation of surface depressions. It can be described as the movement of water from a drainage area across the land surface towards lower elevations (Nasiri et al., 2020a). In SWAT, there are two methods to estimate surface runoff: the SCS curve number procedure and the Green and Ampt infiltration method. The SCS curve number method is used in estimating the rainfall-runoff relationship. In this method, the total rainfall is divided into three components: direct runoff (Q), actual retention (S), and initial abstraction (I) (Bridget et al., 2002). Within SWAT, the runoff is calculated independently for each Hydrologic Response Unit (HRU) and then routed to determine the total runoff for each sub-basin. This method allows for a more detailed assessment of runoff generation at the HRU level, which is then aggregated to obtain a comprehensive understanding of the total runoff within the sub-basin. The surface runoff volumes for each HRUs are simulated using the SCS curve number method, which is determined by applying the following equations (Moriassi et al., 2012).

$$Q_{surf} = \frac{(R_{day} - 0.2S)^2}{R_{day} + 0.8S} \dots\dots\dots (2)$$

Within the given equation,  $Q_{surf}$  represents the accumulated runoff or rainfall excess in millimeters (mm).  $R_{day}$  refers to the daily rainfall depth in mm. The retention parameter, denoted as S, varies spatially due to factors such as soil characteristics, land use, management practices, and slope. Additionally, it also varies temporally based on changes in soil water content. The calculation for the retention parameter is determined using the following equation (3).

$$S = 25 \cdot 4 \left( \frac{100}{CN} - 10 \right) \dots\dots\dots (3)$$

Where CN is curve number

### **C. Evapotranspiration**

Evapotranspiration involves the combined processes of evaporation and plant transpiration, representing the transfer of water from the Earth's land surface to the atmosphere. Evaporation primarily involves the movement of water molecules from various sources, including the soil, canopy interception (such as water retained on leaves), and water bodies like lakes or rivers, into the atmosphere. Evaporation plays a significant role in the water cycle as it contributes to the overall loss of water from the Earth's surface. It occurs when heat energy from the Sun causes water molecules to gain enough energy to transition from a liquid to a vapor state. The vaporized water molecules then ascend into the atmosphere, where they contribute to the moisture content and eventually form clouds. SWAT employs three distinct methods (Scanlon et al., 2002d) to calculate actual evapotranspiration (ET) and potential evapotranspiration (PET): Priestley Taylor, Hargreaves, and Penman-Monteith. These methods offer valuable insights into how climate variations, particularly rising temperatures, can impact water resources.

The Penman-Monteith method, chosen for this study, relies on multiple factors including solar radiation, air temperature, relative humidity, and wind speed to estimate evapotranspiration accurately. On the other hand, the Priestley Taylor method considers solar radiation, air temperature, and relative humidity, while the Hargreaves method relies solely on air temperature (Banimahd et al., 2017). Understanding of evapotranspiration is crucial for comprehending the potential effects of climate change on water resources. By utilizing the Penman-Monteith method, which incorporates several key climatic variables, SWAT enables a more comprehensive assessment of evapotranspiration dynamics and their implications. This knowledge is essential for managing and planning water resources effectively in the face of changing climatic conditions.

#### D. Groundwater Recharge

Aquifer recharge transpires through the processes of percolation and bypass flow, where water moves from the soil surface through the vadose zone and eventually replenishes the aquifers. The time it takes for water to exit the soil profile and enter the aquifer as recharge relies on various factors, including the hydraulic properties of the geological materials within the vadose and groundwater zones, as well as the depth of the water table. In SWAT, the calculation of aquifer recharge includes an exponential decay weighting function. To accommodate the time lag between water departure the soil profile and recharging the aquifer. This approach, as described by allows for a more accurate representation of the temporal dynamics associated with aquifer recharge in the model(Neitch et al., 2005).

$$W_{rchg,i} = (1 - \exp[-\frac{1}{\delta_{gw}}]) \cdot W_{seep} + \exp[-\frac{1}{\delta_{gw}}] \cdot W_{rchg,i-1} \dots \dots \dots (4)$$

Where:  $W_{rchg,i}$  is the amount of recharge entering the aquifer on a day  $i$  (mm);  $\delta_{gw}$  is the delay time or drainage time of the overlying geologic formations (days);  $W_{seep}$  is the total amount of water exiting the bottom of the soil profile on the day  $i$  (mm); and  $W_{rchg,i-1}$  is the amount of recharge entering the aquifer on day  $i-1$  (mm).

## **CHAPTER THREE**

### **3. DESCRIPTION OF THE STUDY AREA**

#### **3.1 Location and accessibility**

The Wabe Shebele River basin, located in Ethiopia, is one of the twelve major basins in the region. It holds the distinction of being the largest basin, covering a substantial total area of 202,220 km<sup>2</sup>. The Upper Wabe Shebele watershed is located in the Wabe Shebele River basin in the southeastern part of Ethiopia, approximately 320 kilometers southeast of Addis Ababa. Geographically, the study area stretches between 6°30'0"N and 7°30'0"N latitude and 38°30'0"E to 39°45'0"E longitude (Figure 3.1). It covers an approximate area of 4413 square kilometers, which represents around 2.18% of the total area of the Wabe Shebele River Basin. The area is bordered by the Zeway Shalla basin to the west and northwest, and by the Genale-Dawa basin to the south and southwest. The study area can be accessed by Addis Ababa-Modjo-Shashemene-Bale Robe and Addis Ababa-Adama-Asela-Bale Robe asphalt road. Intra-basin areas can be accessed by numerous gravel and dry weather roads.

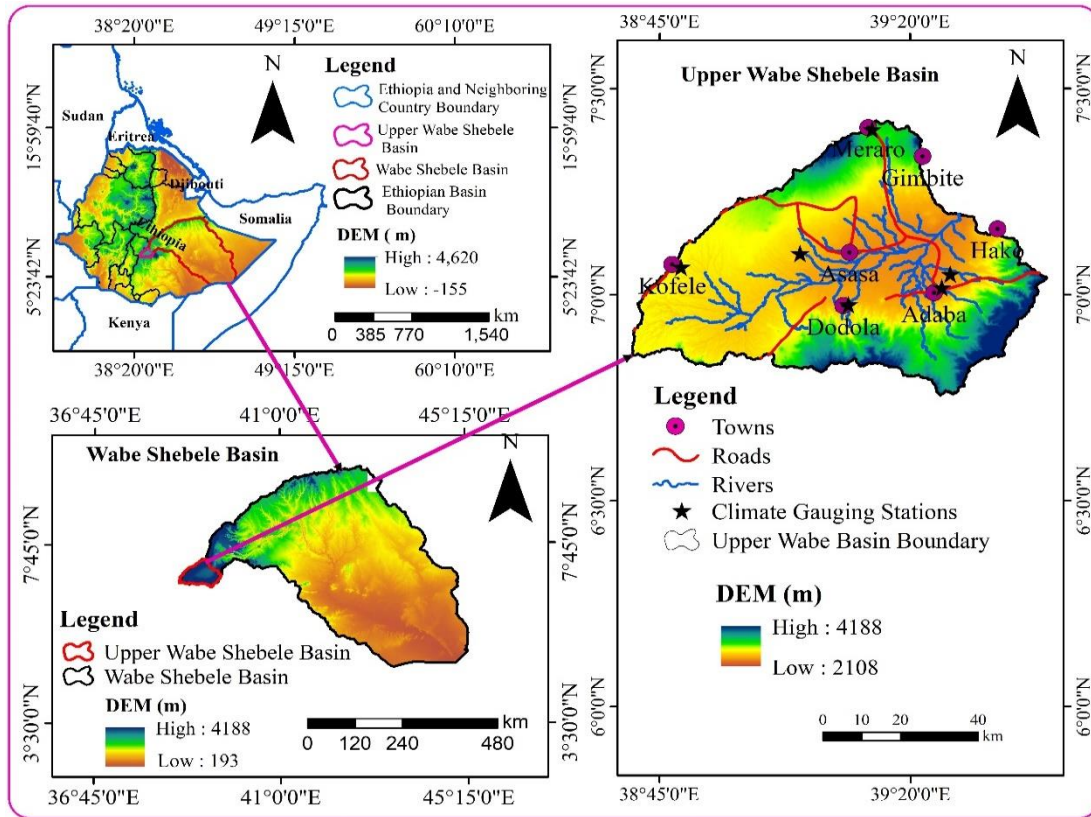


Figure 3.1 Location map of the study area.

### 3.2 Climatic Condition

Ethiopia's climate is mostly shaped by the shifting patterns of the Inter Tropical Convergence Zone (ITCZ), which moves north and south, along with the country's complex topography. The Upper Wabe Shebele river basin exhibits a bimodal rainfall pattern. Most parts of the catchment receive the majority of their rainfall during June, July, August, and September. The rainy season typically begins in March and extends to October, with the highest rainfall concentration occurring in August (Figure 3.2). On average, the catchment receives approximately 961 millimeters of rainfall annually. This watershed experiences temperature variations throughout the year, creating a moderate climate overall. The mean daily temperature usually falls between 13°C and 19°C, and the average monthly temperature ranges from 12°C to 16°C (Figure 3.2).

These temperature ranges contribute to the overall suitability of the catchment area for a variety of fauna and flora.

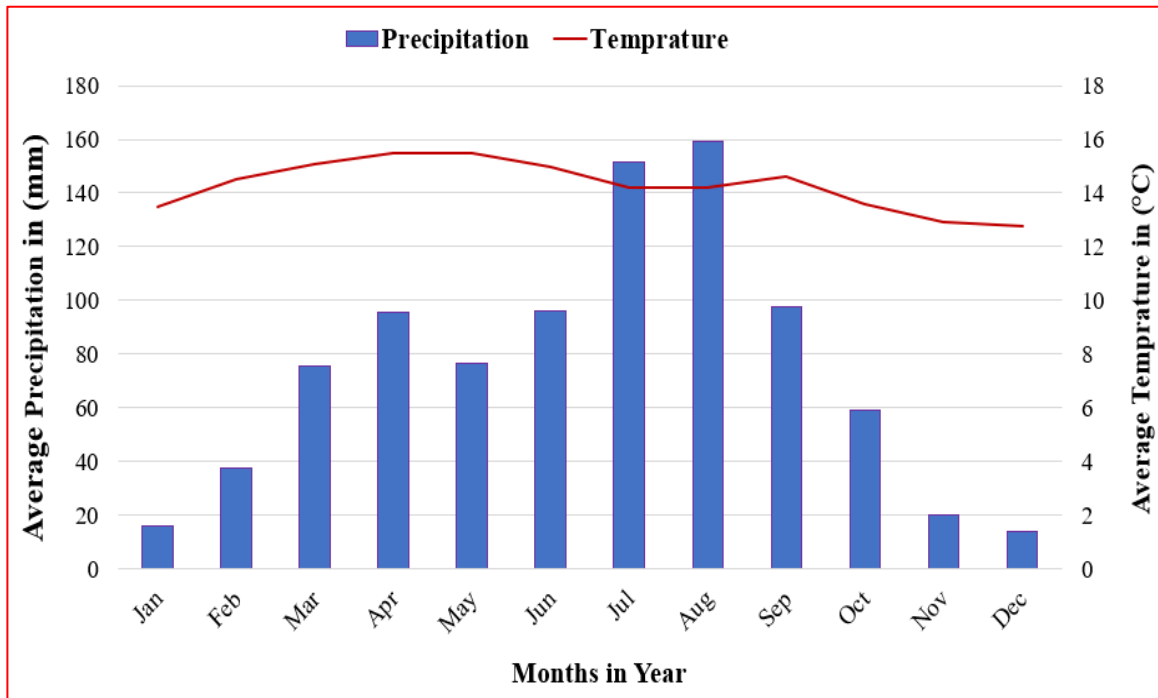


Figure 3.2 Average monthly climate distribution across six stations (Adaba, Ardayita, Dodola, Hunte, Kofale, and Meraro) in the study area.

### 3.3 Drainage

The Wabe Shebelle River travels in a southeastern direction from the mountains located on the eastern rift shoulder. It then passes through the Gedeb plain before entering a steep and deep canyon. The drainage pattern of upper Wabe Shebele river basin primarily relies on rock and soil formations, topography, climate, and the intensity of surface and sub-surface fractures. The relief configuration of the study area, along with its surrounding areas shaped by geological events in the past, determines the flow direction of the rivers. All the rivers in the watershed ultimately drain into the Wabe river. The Upper Wabe river is fed by several tributaries, including Asasa, Furuna, Leliso, Maribo, and Ukuma. These tributaries flow constantly throughout the years. The study area exhibits a dense drainage system characterized by parallel, sub-parallel, and dendritic drainage patterns that ultimately flow into the Wabe river located in the central part of the watershed (Figure 3.3).

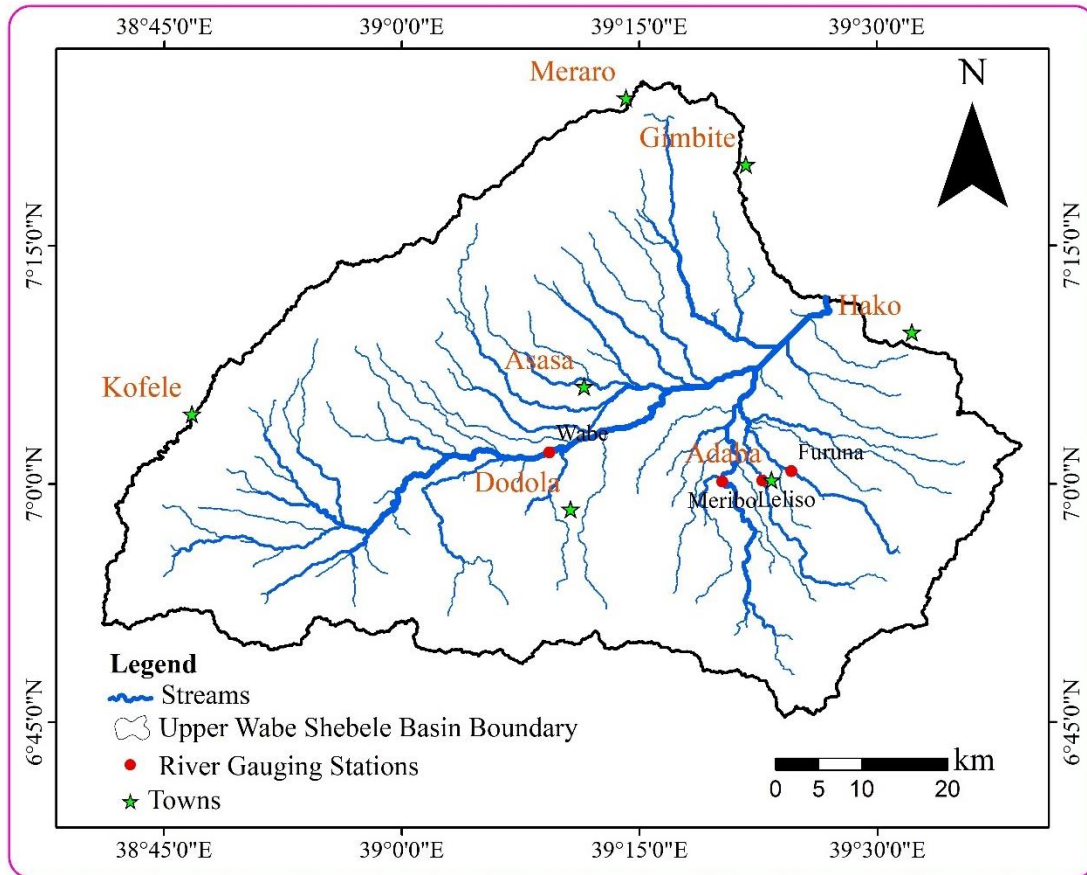


Figure 3.3 Drainage map of study area

### 3.4 Physiography

The physiographic features of the study area are shaped by volcanic mountains and cones along the borders, which display rugged topography. In contrast, the central region consists of volcanic plains characterized by flat land with minimal elevation differences. The watershed's topography changes as it moves from the mountainous highlands in the north and south to the steep gorges where the basin exits the region. The surface elevation of the basin ranges from approximately 2000 meters above sea level at the central plateau and gradually increasing to around 4200 meters near the Bale Mountains in the south and the Kaka and Honkolo mountain in the north (Figure 3.4). The variation in topography led to the formation of distinct climatic zones that align with different physiographic features. The plateau regions receive comparatively higher levels of rainfall in contrast to the lowland areas. As a result, the landscape suffered by erosion and significant changes, causing the transportation and deposition of the eroded sediments along the river valleys' banks.

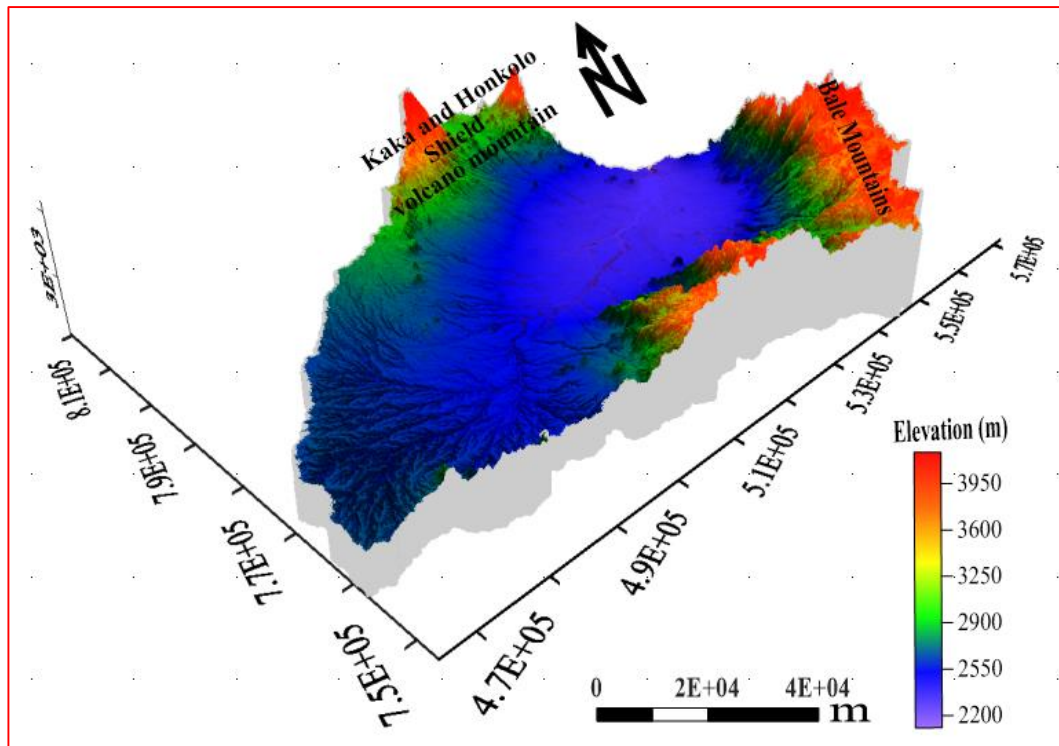


Figure 3.4 Physiographic map of study area

### 3.5 Regional Geology

Ethiopia's diverse landscapes are shaped by tectonic, erosive, and depositional processes, resulting in a unique geological history marked by mountain-building, uplift, fault activity, and lava flows. The country features a high plateau divided by the Rift Valley into two main highland regions: the northwestern and southeastern highlands. Elevation varies dramatically, from Asal Lake, the lowest point in Africa at -150 m, to Mt. Ras Dejen, which reaches 4,620 m (Billi, 2015). Ethiopia's geography can be categorized into four main physiographic regions: 1) Western Plateau: High plateaus (1,500 to 4,620 m) that are the source of major rivers. 2) Southeastern Plateau: Rugged landscapes (1,500 to 4,200 m) with national parks and wildlife reserves. 3) Main Ethiopian Rift: A series of valleys and lakes notable for their unique biodiversity, and 4) Afar Depression: A low-lying desert basin below sea level, known for extreme heat and geological features such as volcanoes and hot springs. The Ethiopian plateau, influenced by tectonic activity related to the Afro-Arabian Shield, consists of various rock types

from different geological periods, including Precambrian metamorphic and Tertiary volcanic rocks (Workineh et al., 2014).

In geological context, there are occasional instances of sedimentary rocks from the Late Paleozoic to Early Mesozoic periods, which provide a basis for the extensive sedimentary sequence of the Mesozoic era (Workineh et al., 2014). In the Bale region, the Cenozoic volcanic formations are divided into four primary groups, which together form a sequence of basalts and trachytes. These groups include the Lower Stratoid Basalts, Reira Basalts, Dodola and Aroresa Trachytes, and Sanete Basalts along with Batu Trachyte. This Cenozoic volcanism features both flood basalts and bimodal basalt-rhyolite/trachyte-pyroclastic activity, occurring from the Tertiary to the Quaternary periods (Workineh et al., 2014). The Cenozoic Volcanic Provinces of Ethiopia offer a helpful structure for classifying the Tertiary volcanic formations in the region. These formations are primarily divided into two main categories: the Pre-Rift (trap) Series and the Rift Series (Zanettin et al., 2006). The Pre-Rift (trap) Series consists of volcanic formations that occur before the rift develops. These formations feature extensive lava flows called traps and mainly consist of basaltic lavas along with related volcanic materials, such as pyroclastic deposits. In Ethiopia, this series includes the Alaji Volcanics, which can be split into two units: Alaji Basalt and Trachyte. The Alaji Basalt is often referred to as the Lower Trap Series, Lower stratoid basalt, and Lower aphyric to porphyritic basalt (Berhe et al., 1987; Workineh et al., 2014).

The Alaji basalt, a major component of the rock unit, mainly consists of aphyric to locally porphyritic basalt and can attain a thickness of up to 800 meters. In many areas, it unconformably overlies Mesozoic sedimentary formations. In contrast, the Rift Series includes volcanic formations that are intimately connected to the rift's development. These volcanic rocks are directly related to the tectonic processes and geological changes occurring within the rift system. They exhibit an unconformable relationship, lying above the Pre-Rift (trap) series volcanics. Between the Rift Series and the underlying Pre-Rift volcanics is a sedimentary layer known as the Chorora sediments. This layer represents a time span of 7 to 10 million years and can reach a maximum thickness of 60 meters (Berhe et al., 1987).

### **3.6 Local geology**

The geology of Upper Wabe Shebele river is mainly composed of Cenozoic volcanic rock (Figure 3.5). The Cenozoic volcanism within the study area region preserves a document of flood basalts and bimodal basalt-rhyolite/trachyte-pyroclastics volcanism spanning from Tertiary to Quaternary. The Tertiary volcanic rocks are divided into Pre-Rift (trap) collection and Rift-collection.

#### **3.6.1 Nazreth Group and Dino Formation**

The western part of the study area comprises a significant deposition of Nazreth Group and Dino Formation. These formations show a distinct boundary, characterized by a sharp contact, with Alkali trachyte flows. As move towards the east, there is minor alkali trachyte tuffs and basalt, along with plugs, upper pyroclasts, and highland basalt bordered this unit within the study area (Workineh et al., 2014). On the southern side and neighboring the area, there are middle basalt porphyritic basalt formations. This geological formation contains various lithological units, including ignimbrites, rhyolites, and basalts. This rock unit is also characterized by having scoria cones: that mainly constitutes layered, gentle sloping beds of gravelly, pinkish scoria fall. These scoria cones formed subrounded hills or cones.

#### **3.6.2 The plateau basalt**

In the study area, plateau basalt is located around the eastern border. It is surrounded by highland basalt flows to the north and south, and upper pyroclasts to the east within the study area. The area is primarily a tableland, and the slopes are nearly horizontal.

#### **3.6.3 The upper pyroclasts**

The upper pyroclasts, previously known as the Nazreth series, form a significant geological feature covering a vast plateau in the central part of the study area, extending from Asasa to the Malka Wakana hydroelectric power station. This region is characterized by a diverse array of pyroclastic materials, which include ignimbrites, ash-fall tuffs, gravelly ash, ash-fall deposits, volcanic breccias, and normal tuff. Each of these components reflects the area's volcanic history and contributes to the overall geological complexity. Ignimbrites, for instance, are typically formed from the deposition of volcanic ash during explosive eruptions. The upper pyroclasts is strategically situated, bordered by several notable geological formations. To the east, the unit is flanked by the Nazret and Dino formations, to the north, highland basalt flows. The western

boundary features plateau basalt and highland basalt, which further illustrate the volcanic history and the interplay of different geological processes. To the south, the presence of trachytic tuffs, along with minor basalt and alkali trachyte flows, indicates a variety of volcanic activity that has occurred over time.

#### **3.6.4 The highland basalt flows**

The northern highlands of the Arsi plateau and the southern highlands of the Bale Mountains, extending to the Hako highlands, are composed of Highland basalt. These basalt formations, resulting from central eruptions, are prominently exposed above upper pyroclastic deposits. In the study areas specifically around Serbo, northeast of Meraro, and the eastern part of Hunte—these lava flows are prevalent (Workineh et al., 2014). They create expansive plateau regions and are characterized by their young, fresh basalt composition.

#### **3.6.5 Alkali trachyte flows with some plugs**

The Alkali trachyte flows with some plugs in the southern part of the study area is interbedded with different geological units. This unit is creating prominent plateau surfaces that stretch from Adaba to Dodala. The alkali trachyte flows unit is bordered by trachytic tuffs, which include minor basalt and alkali trachyte flows. To the south, the unit features bordered by interlayered alkali trachyte and basalt flows. This area appears to be characterized by minimal dissection, indicating that it hasn't been significantly shaped by erosion or geological activity. The slopes suggest a relatively flat landscape, which could be typical of plateaus or certain types of plains.

#### **3.6.6 Trachytic tuffs with minor basalt and alkali trachyte flows and sediments**

The Trachytic tuffs, along with minor basalt and alkali trachyte flows and sediments, were extensively deposited across a significant area. This area spans from the Nazret Group and Dino formations in the west, to the alkali trachyte flows in the south, and the upper pyroclasts in the north within the study area.

#### **3.6.7 Interlayered alkali trachyte and basalt flows**

Interlayered alkali trachyte and basalt flows is deposited on highland of the southern border study area, there is a vast flat-topped region composed of alkali trachyte and basalt flows. These flows stretch approximately in an east-west direction. It consists of intricately interlayered alkali trachyte and basalt flows, with the trachyte being slightly more dominant. In the western and central parts of this unit, there are common occurrences of alkali trachyte plugs. his unit is

bordered to the north by Alkali trachyte flows and to the northeast by highland basalt flows in the study area.

### **3.6.8 Pliocene basalt flows**

In the highland areas around Kaka mountains northern edge of study area, the Pliocene basalts were exposed, mainly located at the foot of the mountain peaks. These basalts form the foundational layer beneath the highland basalt and are covered by Pliocene trachyte flows. Characterized by their fresh, compact, massive, and dense nature, the Pliocene basalts usually exhibit a color spectrum from grey to dark grey (Gobena et al., 1997). Their unique composition and structure set them apart in the region's geological landscape.

### **3.6.9 Pliocene trachyte flows**

Within the study area, the summit regions of Kaka, and Bale Mountain are characterized by the presence of trachyte flows. These flows, known as Plio-Pleistocene trachyte flows, are relatively young and belong to the post-rift central type. The trachyte flows are light grey in color, exhibiting slight weathering. They possess a fine to medium-grained texture and occasionally display porphyritic features, with sanidine phenocrysts visible in some areas (Workineh et al., 2014). This unit occupy a relatively small portion of the study area.

### **3.6.10 Quaternary alluvial deposits**

Within stream valleys, a diverse range of materials including talus, rock debris, and silty soil have been deposited as Quaternary alluvial sediment. These sediments accumulate along the valley floor and collectively form a detailed mapping of the alluvium deposits. In the study area, this unit is specifically deposited in a small area at the border of the river.

### **3.7 Geological Structure**

Geologic structures are the essential features created during the formation of rocks (primary structures) and those that develop after rock formation (secondary structures). For the current study area secondary structures include lineaments, joints, and fractures, were largely linked to the extensional tectonics of the MER are dominant. A series of lineaments trending east-west, northeast, and north-south-southwest intersect the area, with east-west lineaments being the most prevalent. These lineaments were extracted from satellite images using Geomatica 2018 software. The overall orientation of these lineaments roughly aligns with the local drainage systems. While the lineaments are spread throughout the study area, they are more densely concentrated in the western, northern, southeastern, and southwestern regions (Figure 4.1). Lineaments primarily influenced by the upper pyroclastic identified in the Gedeb-Asasa plain and it is sparsely distributed in these regions. Consequently, these fractures appear to play a significant role in the storage and movement of groundwater in the catchment. This watershed is also characterized by scoria cones. It primarily consists of layered, gently sloping beds of gravel scoria deposits, which form subrounded hills or cones.

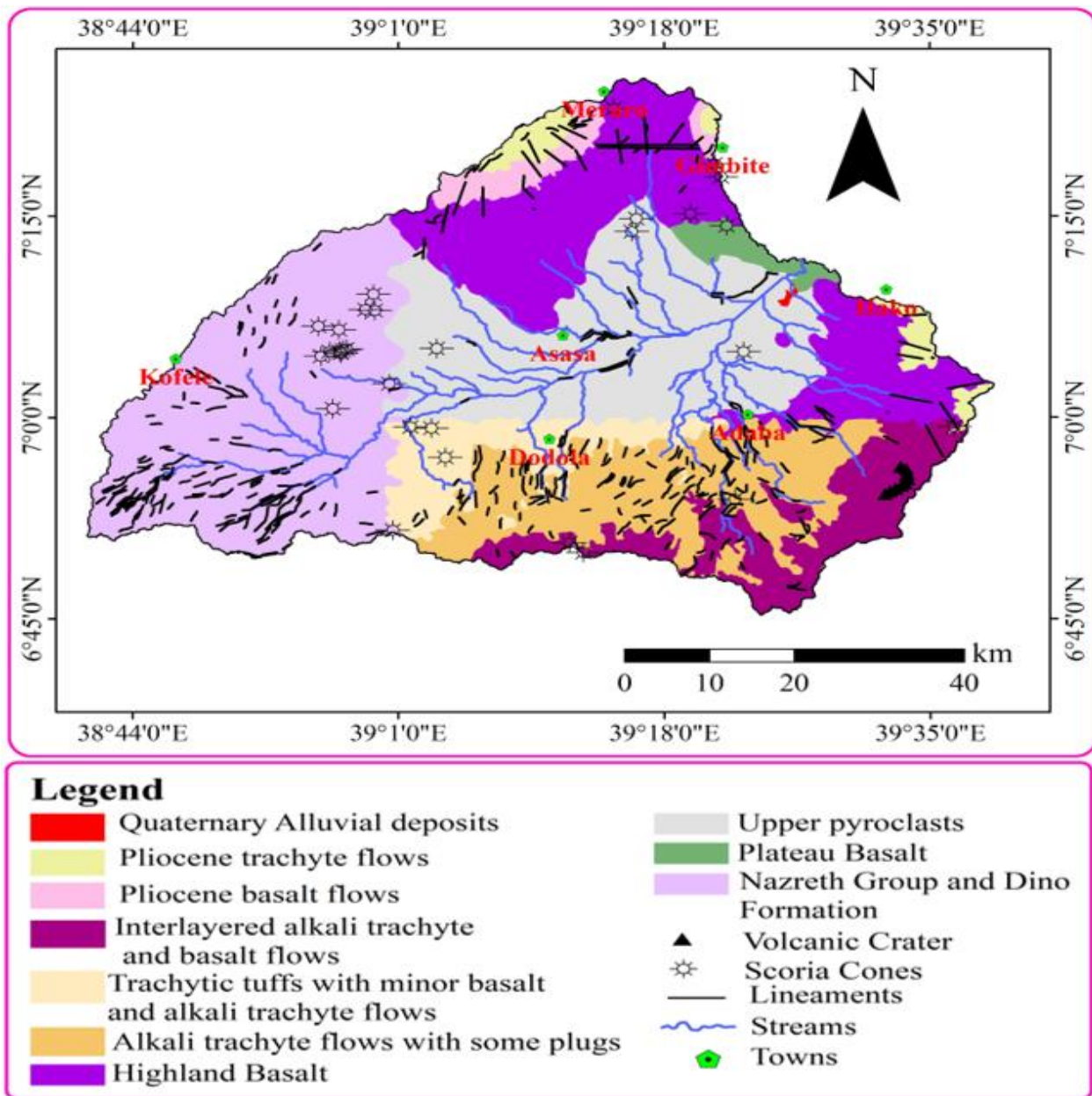


Figure 3.5 Geological map of Upper Wabe Shebele river basin and distribution of the lineaments in the region (adapted from (Alemayehu et al., 1991; Aman et al., 2012; Basalfew et al., 2012; Workineh et al., 2013)).

## **3.8 Hydrogeology**

### **3.8.1 General**

The hydrogeological characteristics of Wabe Shebele river basin are influenced by several major factors, including the nature of the geological formations, the regional and local structural conditions, the geomorphology and landforms, the climatic conditions (often interconnected with the topography), the land-use and land-cover patterns, and other relevant elements (Kebede, 2013). There are two major factors contributing to the groundwater occurrence in the study area: the E-W and SE-NW trending mountain ranges, which are stretched along the water divide between Awash, the Rift Valley Lakes and the Genale-Dawa Basins. These mountains collect part of the rainfall and recharge the groundwater. Excess precipitation infiltrates volcanic formations, covering mountain ranges and percolating into underlying or saturated formations. Groundwater emerges as springs at outcrop areas, topographic changes, and fracture intersections, with varying outflow rates based on natural characteristics and inflow conditions. The hydrogeological configuration of the study area is categorized based on the hydrogeological characteristics, specifically the water-bearing capacity and permeability dynamics of the geological formations.

#### **Aquifer Type**

The aquifer types in this specific study area are classified into five categories based on the porosity and permeability of the geological materials: 1) Extensive and Highly Productive Fractured and/or Porous Volcanic Aquifer, 2) Extensively Developed Medium to High Productive Fractured, Jointed, and Porous Aquifer, 3) Extensive and Moderately Productive Fissured Aquifers, 4) Extensively Developed Low to Medium Productive Fractured Aquifer, and 5) Extensive and Low Productive Fractured Volcanic Aquifer. This classification reflects the varying productivity levels of the aquifers present in the study area.

### **3.8.2 Extensive and High Productive Fracture and/or Porous Volcanic Aquifer**

A fractured, jointed, or porous volcanic aquifer system is found within the Tertiary Volcanics of the Nazret Series and upper pyroclasts. This aquifer unit covers an area of 2171 km<sup>2</sup>, representing 49% of the total aquifer system in the study area. The aquifer features varying types of permeability, including intergranular and fractured permeability. Shield volcanoes

feature a unique combination of acidic lava, ash, and fractured basalt layers that facilitate groundwater storage and movement. In shield volcanoes where lava alternates with air-fall ash, two-part aquifer systems have been observed through high-yield spring discharge (Kebede, 2013). In addition to their geomorphic significance for groundwater dynamics, the lava flow structure identifies shield volcanoes as hydrogeological units compared to the underlying flood basalt plateau, with thinner, less continuous lava flows contributing to the frequent emergence of springs within shield volcano areas. The Assasa Spring, located at the foothills of the Arsi-Bale Mountains east of Mountain Kaka in southeastern Ethiopia, is one of the largest recorded springs in the country, with a discharge rate of 500 liters per second (Kebede, 2013). This remarkable multiple-eye spring supplies water to Assasa, Dodola, Ardayita College, and nearby villages. Additionally, it serves as a significant tributary of the Wabe River. In this aquifer, boreholes range in depth from 35 to 153 meters, yielding between 0.33 l/s and 5.6 l/s. The static water levels vary from artesian conditions to 80 meters below the surface, with an average of 33 meters (Astatke et al., 2009).

### **3.8.3 Extensively developed medium to high productive, fractured, jointed and porous aquifer**

The aquifer system comprises various rock types, including basalt, which is often characterized by a scoriaceous texture. It also includes alkali trachyte flows and minor plugs (Tpt), interlayered alkali trachyte and basalt flows (Tbt), trachitic tuffs with minor basalt and alkali flows, and sediments (Tps). Additionally, the system features aphyric basalt (Tab), alkali trachyte flows with some plugs, minor alkali trachyte tuff, and basalt (Ttr), as well as aphyric and porphyritic basalt (Kiflu, 2010). The Upper Wabi Shebele basin contains areas covered by this aquifer type, which exhibits an average discharge of 5.74 l/s. In the study area, this aquifer extends from the western region of Dodola to the northeastern vicinity of Adaba town. This aquifer unit covers an area of 397km<sup>2</sup>, representing 10% of the total aquifer system in the study area.

### **3.8.4 Extensive and Moderately Productive Fissured Aquifers**

Fissured aquifers with moderate productivity cover a small area, specifically around the western edge and northwestern part of the study region. These aquifers are primarily composed of basalts, rhyolites, trachytes, ignimbrites, and tuffs, although they are not individually mapped. Basalt formations typically produce less viscous and thin lava flows that can experience significant weathering and brecciation, often interbedded with lacustrine or fluvial deposits. Groundwater movement occurs through various pathways, including joints, fractures, scoria intercalations, coriaceous horizons, and interbedded sediments. The presence of both horizontal and vertical fractures ensures hydraulic continuity within the aquifers and facilitates connections with neighboring units, leading to the development of low to medium productive fractured and foliated aquifers. (Agezew et al., 2014). This aquifer unit covers an area of 81km<sup>2</sup>, representing 1.84% of the total aquifer system in the study area.

### **3.8.5 Extensively developed low to medium productive fractured aquifer**

This aquifer system is the second largest by area, encompassing the entire study region. This aquifer unit covers an area of 1525km<sup>2</sup>, representing 33.81% of the total aquifer system in the study area. It has an average discharge of 0.7 l/s. The geological materials that make up this aquifer in this study area include highland basalt, trachytic tuff with minor basalt, alkali trachyte and Interlayered alkali trachyte and basalt flows (Astatke et al., 2009). This aquifer system is primarily located in the southern and northern sections of the project area.

### **3.8.6 Extensive and Low Productive Fractured Volcanic Aquifer**

Extensive and Low Productive Fractured Volcanic Aquifer unit covers an area of 236km<sup>2</sup>, representing 5.35% of the total aquifer system in the study area. The southeastern plateau of Ethiopia features a flood basalt succession marked by rugged topographic units intersected by the Wabe Shebele River. Within the study area, there is a small low-productivity fractured volcanic aquifer comprised of two formations: the Arsi Bale basalt (PNa1) and the Alkali Trachyte flow (PNa2). The Alkali Trachyte flow (PNa2) contributes to the formation of wide ridges with gentle to steep sides and flat tops.

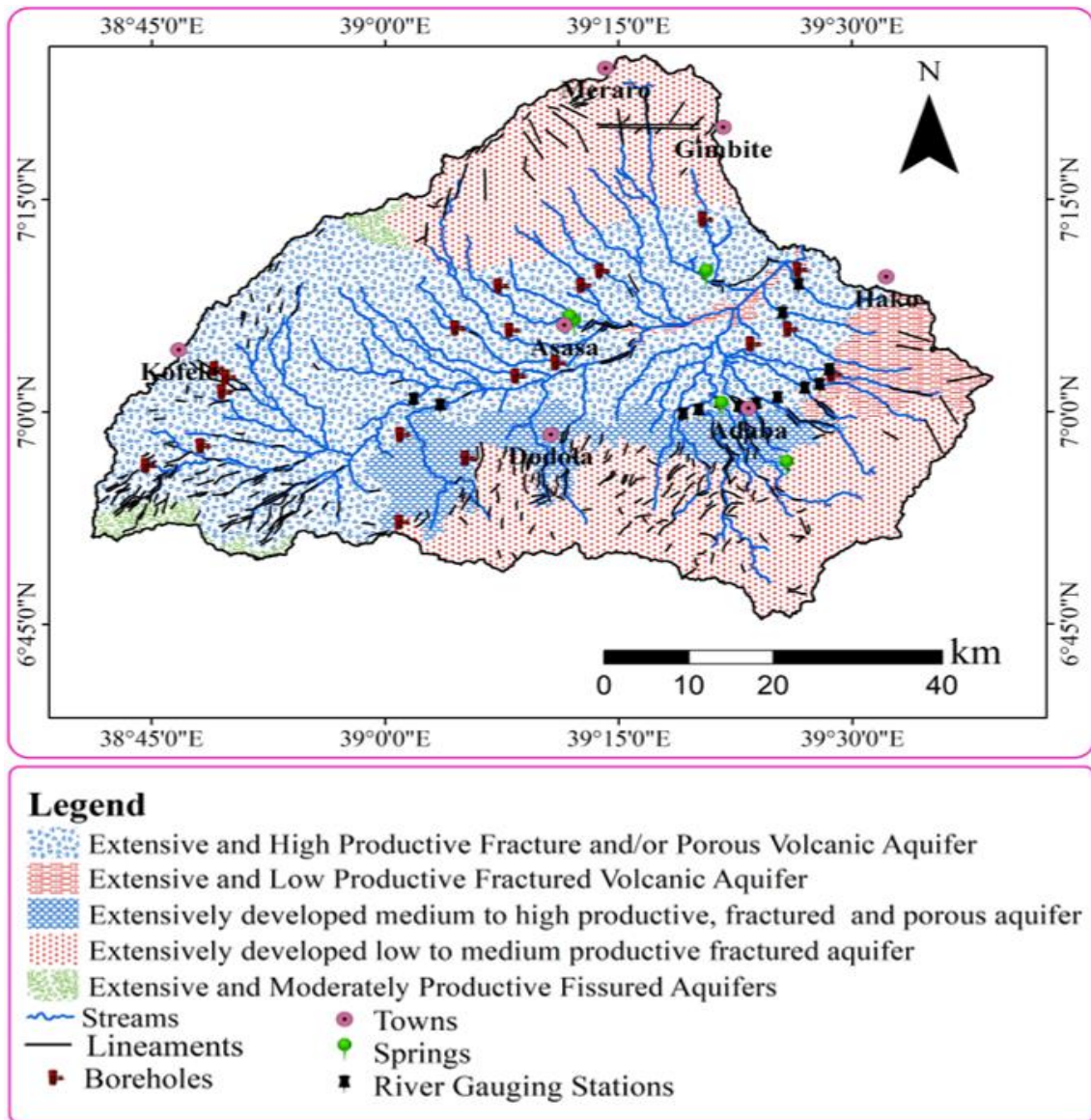


Figure 3.6 Hydrogeological map of Upper Wabe Shebele basin (adapted from (Agezew et al., 2014; Astatike Kiflu & H/Mariam, 2010; Astatke et al., 2009; Kiflu, 2010; Tilahun & Sima, 2013)).

### **3.9 Ground Water Flow, Recharge and Discharge**

The presence and flow of groundwater in volcanic rocks are primarily controlled by the porosity and permeability characteristics that develop during and after the rock's formation. Due to the topography of the study area, the direction of groundwater flow closely follows the same path as surface water flow. This alignment is largely influenced by the landscape's features, such as hills, valleys, and slopes, which shape how both groundwater and surface water move through the environment (Astatke et al., 2009). In many cases, groundwater divides boundaries that separate different groundwater flow systems are assumed to coincide with surface water divides, which are the high points that direct surface water into different drainage basins.

This relationship suggests a strong connection between the two systems; as precipitation falls, it can either infiltrate the ground to become groundwater or flow over the surface, depending on the slope and soil conditions. The flow and storage of groundwater in volcanic rocks are influenced by several key features: Vertical permeability resulting from primary and secondary fractures, horizontal permeability created by layers with openings from lava flow and gas expansion during solidification, presence of impermeable layers and dikes. Fractured and porous volcanic rocks do not always facilitate groundwater circulation (Astatke et al., 2009). The main controlling factors in this context include: The type, frequency, and distribution of fractures, the degree of interconnection between fractures and pores and the thickness of the lava flow.

Groundwater recharge is influenced by several factors, including prevailing temperatures, amount of precipitation, land terrain (slope gradients), the types of rocks (permeability), and land cover (vegetation). In the study area, rainfall is the primary factor influencing groundwater recharge, with precipitation being affected by altitude. The potential aquifers in the area receive recharge from both direct precipitation and runoff from streams. Because most of the volcanic formations are columnarly jointed and fractured, the aquifers on the plateau contribute to the recharge of the underlying volcanic aquifer (Astatke et al., 2009).

Naturally elevated topographical regions are typically regarded as recharge areas, as they facilitate the collection and infiltration of precipitation. These highlands allow water to enter into the ground, replenishing the aquifers below. In contrast, lower-lying areas are often viewed as discharge zones, where groundwater emerges to the surface, feeding streams and rivers. This dynamic interplay between recharge and discharge is crucial for maintaining the hydrological balance in the region. Groundwater discharge manifests as springs in elevated regions and seepages in the valleys (Astatke et al., 2009). Additionally, the steep slopes and escarpments of Wabe contribute to this process by facilitating the movement of water from underground sources to the surface.

# CHAPTER FOUR

## 4. METHODS AND MATERIALS

### 4.1 Desk study

The research involves conducting a comprehensive literature review of hydrological modeling on a global scale, focusing particularly on evaluations within Ethiopia and the designated study region. This includes analyzing published and unpublished paper, reviews, and theories used to assess and quantify the groundwater recharge rates by using the SWAT model. Based on the information collected from the literature review, a conceptual framework and a general methodological flowchart are being developed.

### 4.2 Data Collection

Data essential for estimating groundwater recharge using the SWAT model was gathered from multiple organizations, including the Ethiopian Ministry of Water and Energy, the National Meteorological Service Agency, US Geological Survey (USGS), and the Food and Agriculture Organization (FAO). This data collection phase encompassed a variety of information, such as meteorological data, streamflow records, soil characteristics, and land use/land cover maps. Drawing from the insights gained during the literature review, a comprehensive methodology was developed to analyze this data effectively.

### 4.3 SWAT Input Data Preparation and their Sources

The accuracy and effectiveness of any modeling system, including the Soil and Water Assessment Tool (SWAT), heavily rely on the quality and reliability of the input data utilized during the modeling process. In the case of setting up the SWAT model for the Upper Wabe Shebele catchment, several key data sets were employed to ensure a robust analysis. These data sets encompass a Digital Elevation Model (DEM), a land use/land cover map, a soil map, slope map, as well as meteorological data. Additionally, stream flow data played a crucial role in calibrating and validating the model performance.

#### **4.3.1 Digital Elevation Models (DEM)**

The Digital Elevation Model (DEM) is the primary input parameter for the Soil and Water Assessment Tool (SWAT) model. It is essential for calculating flow accumulation, slope, stream networks, and watershed delineation. This study utilized 30 m × 30 m resolution DEM data from the SRTM (Shuttle Radar Topography Mission) (<https://glovis.usgs.gov/>). It is obtained from the USGS (United States Geological Survey) website. The raster editor in ArcMap was used to modify the original data. Prior to importing into Arc SWAT, the revised DEM data was projected to WGS1984 UTM Zone 37N using the raster projection option in ArcMap. The elevation variation of the study watershed ranges from 2108 to 4188m above mean sea level.

#### **4.3.2 Land-Use/Land Cover (LULC)**

Within the Soil and Water Assessment Tool (SWAT), the Land Use/Land Cover (LULC) data plays a crucial role in determining both the spatial extent and the hydrological characteristics of different land-use types simulated within each sub-basin (Setegn et al., 2010). The LULC data provides essential information regarding the distribution and classification of various land-use categories within the study area. By incorporating this data into the SWAT model, the tool can allocate specific land-use types to individual sub-basins, enabling a detailed representation of the landscape and its hydrological processes. For this study area LULC information was extracted from Landsat 8-9 OLI/TIRS C2 L2 imageries through a supervised classification in Erda's Imagine 2015. The 2023 LULC images, with a spatial resolution of 30 m, were obtained from the US Geological Survey (USGS) database (<https://glovis.usgs.gov/>) for path 168 and row 055. The study area was then divided into 6 LULC classes using a projection type WGS 1984 UTM Zone 37N. Namely: Agricultural land, Bare lands, Forest, Water bodies, Rangelands, and Urban/Settlements (Figure 4.1).

Table 4.1 Distribution LULC type in the Upper Wabe Shebele River Basin

No	LULC	Area (km <sup>2</sup> )	Area (%)
1	Agricultural land	3021.14	68.46
2	Bare lands	23.83	0.54
3	Forest	575.46	13.04
4	Water bodies	52.07	1.18
5	Rangelands	614.73	13.93
6	Urban/Settlements	125.77	2.80

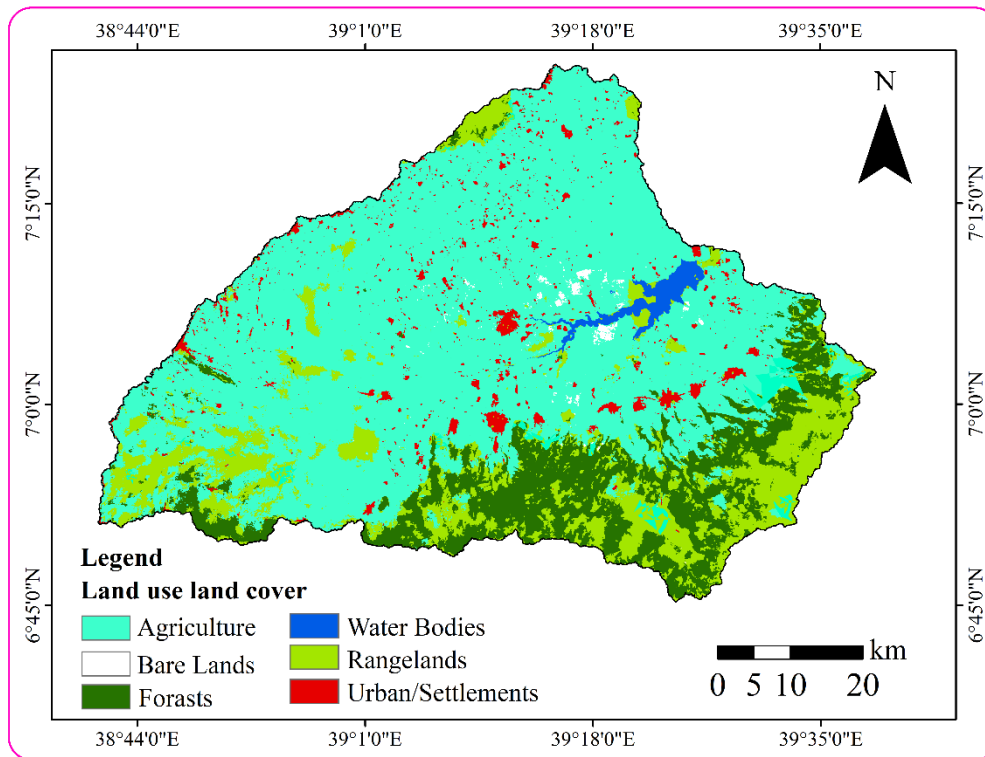


Figure 4.1 LULC map of Upper Wabe Shebele River Basin

### 4.3.3 Soil data

A soil map, including the properties of the soil in the basin, is a crucial input for the Soil and Water Assessment Tool (SWAT) model. For this study, soil data was obtained from the Food and Agriculture Organization (FAO) (<https://www.fao.org/>) and downloaded in ISRI shapefile format for analysis. The data was then projected to WGS1984 UTM Zone 37 to ensure compatibility with other spatial datasets used in the project. To prepare the soil data for further

processing and analysis, it was organized by using ArcMap. This preparation involved standardizing the data format and accurately representing all relevant attributes for SWAT modeling. Although SWAT has its own soil database, new soil characteristics were integrated into the existing SWAT database for this work. According to FAO classification, the study area comprises four major soil types. These are: Vertisols, Humic Nitisols, Cambisols, and Luvisols (Figure 4.2).

Table 4.2 Distribution of soil type in the Upper Wabe Shebele River Basin

<b>No</b>	<b>Soil Type</b>	<b>Area (km<sup>2</sup>)</b>	<b>Area (%)</b>
1	Vertisols	1242.70	28.16
2	Humic Nitisols	435.56	9.87
3	Cambisols	1345.97	30.5
4	Luvisols	1388.77	31.47

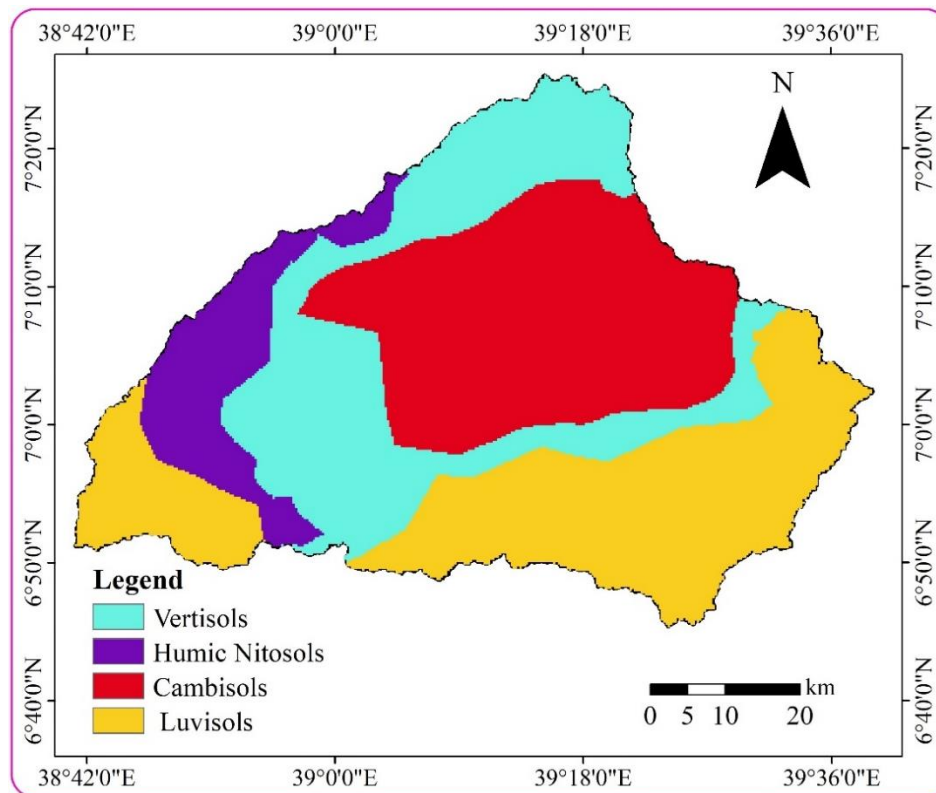


Figure 4. 2 Soil Map of Upper Wabe Shebele Basin

#### 4.3.4 Slope

A crucial step in the watershed delineation process was to classify the slope based on the elevation range derived from the Digital Elevation Model (DEM) utilized in the study. This classification aimed to provide a comprehensive understanding of the slope characteristics within the watershed. To facilitate analysis and interpretation, the slope values were reclassified into percent, offering a standardized measurement by using natural breaks (Jenks) classification method. For this particular study, the slope was divided into four distinct categories based on the specific digital elevation model used. The resulting slope classification is presented below (Fig 4.3).

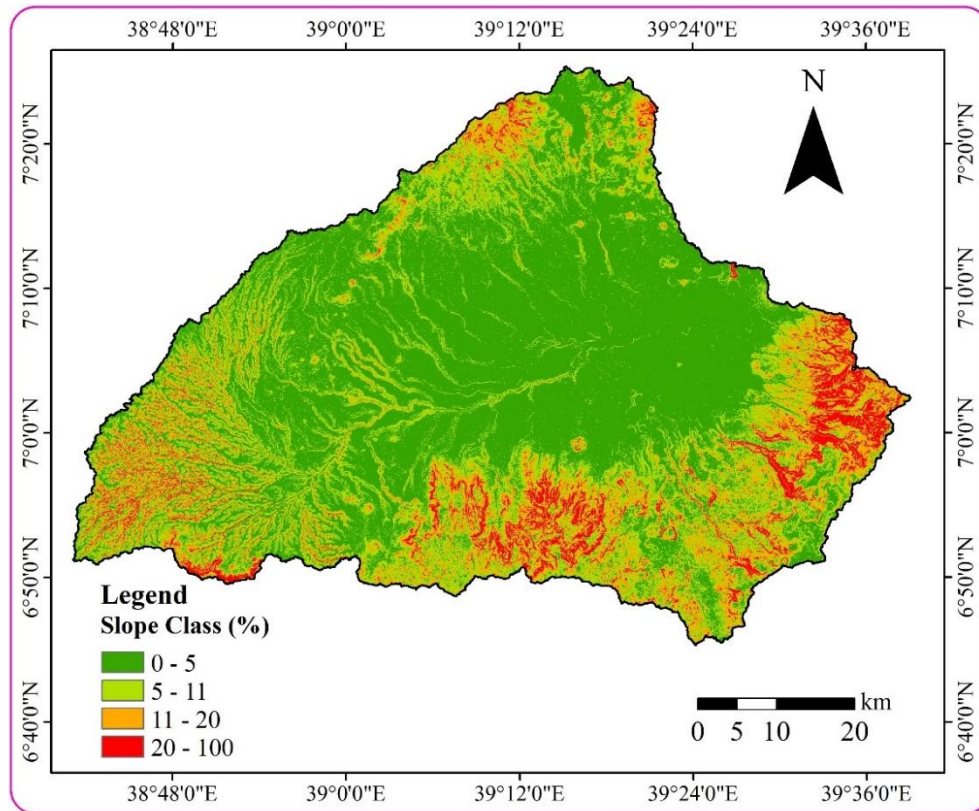


Figure 4.3 Slope map of Upper Wabe Shebele River basin

#### 4.3.5 Climate data

For this study, utilized a comprehensive climate dataset covering a substantial 21-year period from January 1998 to December 2018. This dataset included various meteorological parameters to thoroughly represent the climate system, such as daily precipitation, maximum and minimum air temperatures, relative humidity, wind speed, and solar radiation. The data were sourced from six gauging stations (Adaba, Ardayita, Dodola, Hunte, Kofale, and Meraro) located in the Upper Wabe Shebele River basin. These reliable and localized climate data were obtained from the National Meteorological Agency of Ethiopia, ensuring their relevance to the study area. However, it should be noted that the dataset was not without missing values. To address this challenge, a predictive approach was employed. Arithmetic mean method was utilized to estimate the missing data points based on the available information.

The arithmetic mean, commonly known as the average, is a method that assigns the value at station  $x$  to be equal to the arithmetic average of the values from the three surrounding stations (Stephen, 1999).

$$\bar{x} = \frac{\sum_{i=1}^n x_i}{n} \dots\dots\dots 5$$

Where  $n$  is the number of observations in the sample,  $x_i$  individual sample, and  $\bar{x}$  is the mean of the sample.

By using the relationships between observed data and the missing values, the Arithmetic equations provided as a means to fill in the gaps and create a complete dataset for further analysis. Once the dataset was complete, the weather data was prepared in a specific text file format that adhered to the requirements of the SWAT (Soil and Water Assessment Tool) model. This formatting was necessary to ensure seamless integration of the weather data into the SWAT model, enabling accurate simulations and assessments of the hydrological processes within the study area. The text file format facilitated efficient data input and processing, ensuring compatibility and consistency with the SWAT model's input data requirements.

#### **4.3.6 Stream flow data**

Within the Upper Wabe Shebele River basin, the Furuna, Leliso and Wabe rivers hold significant importance as the three major rivers contributing to its hydrological dynamics. To analyze and understand the behavior of these rivers, daily discharge data covering a substantial period for 21 years from 1998 to 2018 were acquired from the Ethiopian Ministry of Water and Energy. These discharge data served as crucial inputs for both the calibration and validation processes within the Furuna, Leliso, and Wabe sub-watersheds. Upon gathering the discharge data, it was observed that certain time points had missing values, which could potentially hinder the accuracy of the analysis. To address this arithmetic method was employed as a predictive tool. Based on relationships between the observed discharge values and the available data, the Arithmetic method facilitated the estimation and imputation of the missing discharge values. This approach ensured a complete and more comprehensive dataset, enabling robust calibration and validation of the sub-watersheds.

### **4.4 SWAT Model set up**

#### **4.4.1 Watershed Delineation**

The Watershed delineation process was carried out using the step-by-step procedures provided by the Arc SWAT model. The procedure involved several key steps to accurately define the Watershed boundaries and calculate relevant parameters. The first step involved setting up the SWAT project, configuring the necessary inputs, and defining the study area. Following that, the Watershed delineator tool was employed to identify the boundaries of the Watershed based on the specified parameters. Next, DEM-based flow accumulation and direction calculations were performed and enabling the determination of water flow paths within the Watershed. This step helps in understanding the drainage patterns and hydrological processes.

To refine the Watershed boundaries and ensure accuracy, modifications were made to the outlets. Unnecessary outlets were deleted, and additional outlets were added where needed. This step helps in controlling the flow paths and accurately representing the outlets within the Watershed. Once the modifications were made, the selection of the Watershed outlet was determined using specific criteria or user-defined preferences. This helps in identifying the primary outlet through which water exits the Watershed. After the completion of these steps, the

model automatically generates the Watershed of interest, providing a delineated area for further analysis. Following the Watershed delineation, the next step involves calculating the sub-basin parameters, which include various characteristics such as area, slope, land use, and soil properties of the individual sub-basins within the larger Watershed.

By systematically following these procedures, the Arc SWAT model facilitates accurate Watershed delineation and parameter calculation, enabling comprehensive hydrological and environmental analysis within the study area. Using a Digital Elevation Model (DEM) with a spatial resolution of 30m x 30m, the study watershed delineation was done, resulting in the generation of 97 sub-basins. This process involved identifying the river network and dividing the watershed into distinct sub-basin areas. Each sub-basin was assigned a unique basin number, which allows for easy identification and reference. The outcome of the watershed delineation process provides a visual representation of the river network, sub-basins, and their respective basin numbers, offering valuable insights into the hydrological structure of the study area.

#### **4.4.2 Hydrologic Response Units**

To define Hydrologic Response Units (HRUs) land use/land cover (LULC), soil, and slope datasets were imported and integrated with the SWAT databases. This process involved overlaying and linking the datasets to create HRU. For this study, the multiple slope option was chosen to account for different slope classes when defining HRUs. This option allows for a more accurate representation of the landscape's variability and its impact on hydrological processes. To discretize the sub-watersheds into HRUs, threshold values were applied. Specifically, threshold values of 10% for LULC, 20% for soil, and 20% for slope were utilized. These thresholds determined the minimum extent of each parameter required for an area to be considered as a separate HRU. By applying these threshold values, the sub-watersheds were effectively divided into 471HRUs, ensuring that areas with significant differences in LULC, soil types, and slope classes were distinguished as separate hydrologic units. This discretization process enhances the accuracy of hydrological modeling and allows for a more detailed analysis of the watershed's response to different land characteristics.

#### **4.4.3 Weather data definition**

The information collected from weather climate stations located within the Watershed encompasses a comprehensive array of meteorological variables critical for hydrological analysis and modeling. These variables include daily precipitation, minimum and maximum temperature, relative humidity data, wind speed, and solar radiation. To ensure seamless integration into the ARCSWAT model, a widely used tool for watershed-scale hydrological simulations, the collected data was accurately compiled and organized into txt file formats. This formatting choice was made to guarantee compatibility with the specific data input requirements of the ARCSWAT model, allowing for efficient data transfer and utilization within the modeling framework.

#### **4.5 Model uncertainty analysis**

Assessing uncertainty in the SWAT model is vital for reliable hydrological predictions. SWAT-CUP facilitates this through auto-calibration using the SUFI2 method. This process refines model parameters for specific conditions, helping to reduce prediction uncertainty and avoid impractical values. In this work, the calibration of model parameters and the quantification of uncertainty utilized observed streamflow data. The process began with the selection of input parameters to be optimized, followed by decisions regarding the starting and ending simulation numbers. Predefined observed data were inserted according to the requirements of the SWAT-CUP model, and an objective function was defined, typically involving the minimization of the difference between observed and simulated values. The SUFI-2 method was employed for the sequential calibration process, starting with a set of initial parameter values. During each iteration, the model was run, and discrepancies between the observed and simulated data were analyzed. A key characteristic of SUFI-2 is its capability to generate confidence intervals for predicted outputs, offering insights into the reliability of results. After multiple calibration iterations, SUFI-2 yields a set of parameter values that best align with observed data while also providing uncertainty bounds. This method served as a statistical framework to iteratively adjust parameter values, aiming to reduce uncertainty in model outputs. Additionally, conducting sensitivity analyses helps identify critical parameters that necessitate more precise measurement or estimation.

## 4.6 Model Sensitivity analysis

Sensitivity analysis used to assess how different parameters affect model outputs in a watershed, identifying critical factors that influence results. It helps reduce the number of input parameters, cutting down calibration time. This analysis prioritizes which parameters to adjust during calibration. There are two main approaches: local sensitivity testing, which changes one parameter at a time, and global testing, which adjusts all parameters concurrently. Calibrating the SWAT model is challenging due to the many parameters involved, making sensitivity analysis essential for determining their relative importance and guiding calibration efforts (Saltelli et al., 1999). Sensitivity analysis is crucial for effective model calibration, as it identifies parameters that significantly influence model performance. In the Upper Wabe Shebele river basin study, sensitivity analysis was conducted at three gauging stations in the Furuna, Leliso and Wabe river sub-basins to determine critical flow parameters. The SWAT-CUP program, utilizing the SUFI-2 method, automatically identified and ranked these parameters by significance. This systematic approach allows to target their calibration efforts on the most impactful parameters, optimizing the calibration process and improving model accuracy for Upper Wabe Shebele river basin.

This targeted calibration approach improves the reliability and effectiveness of the hydrological modeling for Upper Wabe Shebele river basin and enhances the understanding of its flow dynamics. A total of twenty-one flow-sensitive parameters in (Table 4.3) were chosen for analysis. To assess their sensitivity, 1000 simulations were conducted using River flow data spanning from 2000 to 2011 for all rivers. The ranking of these parameters was determined utilizing global sensitive analyses, employing both p-values and t-statistics. The p-value serves as an indicator of the significance of sensitivity. A p-value close to zero suggests higher sensitivity, while a larger p-value indicates lower sensitivity. On the other hand, the t-statistic measures the magnitude of sensitivity for each parameter (Abbaspour et al., 2007). The parameter with the largest absolute value of the t-statistic is considered the most sensitive. By considering both the p-values and t-statistics, the ranking of the flow-sensitive parameters was established. This ranking aids in identifying the parameters that have the greatest impact on the river flow dynamics and it is crucial for accurate modeling and analysis. Overall, the combination of p-values and t-statistics provides a comprehensive assessment of parameter

sensitivity, enabling to prioritize focus on the most influential parameters for further analysis and calibration in the context of river flow modeling.

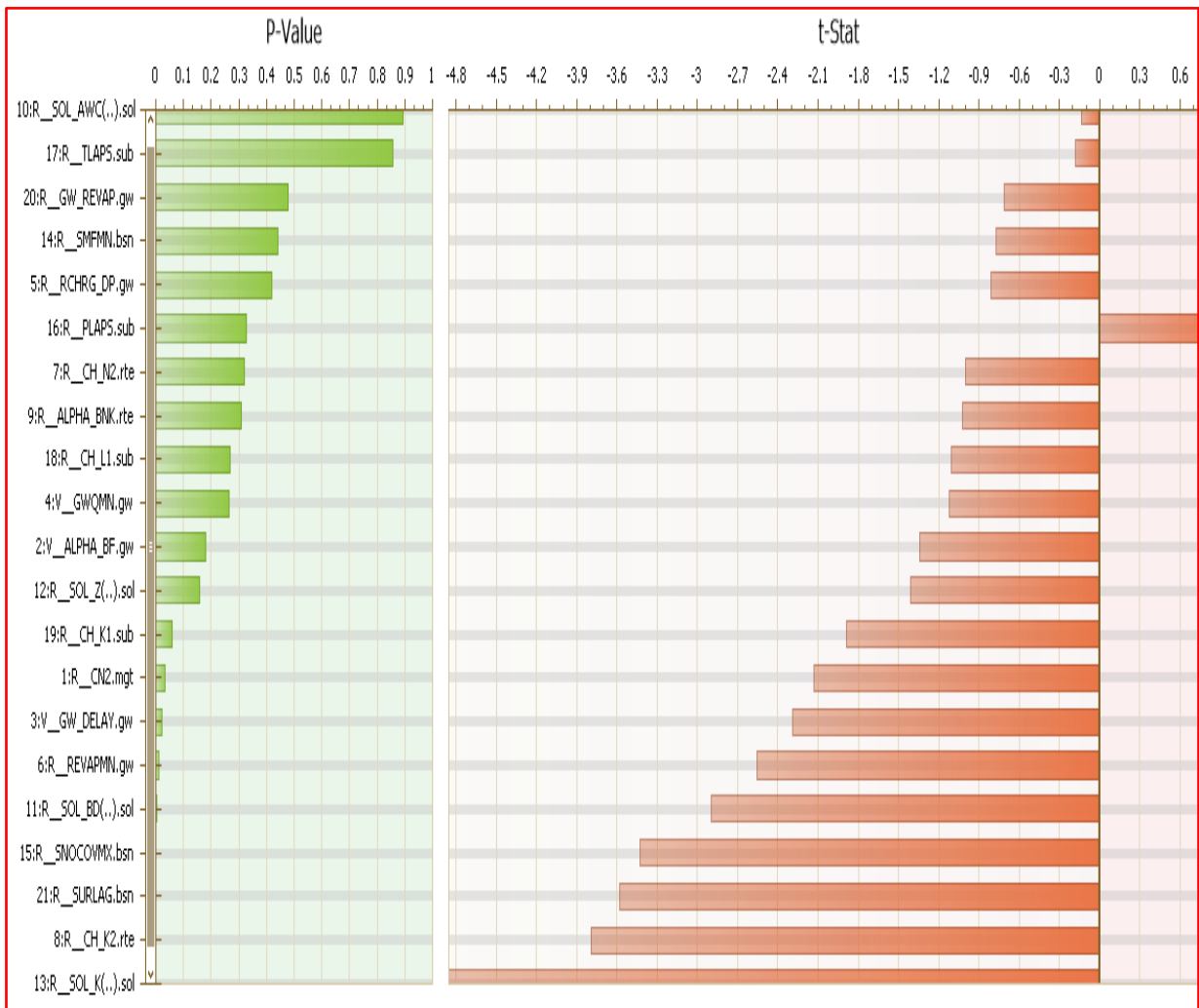


Figure 4.4 Sensitivity analysis using SWAT-CUP based on t-stat and p-value

The SWAT CUP analysis of the global sensitivity option involved a thorough assessment of multiple parameters, resulting in a comprehensive list. These parameters were carefully ordered based on their increasing sensitivity. This ranking provides valuable insights into the relative importance of each parameter in influencing the model's outputs.

Table 4.3 Sensitive flow parameters and their Calibrated range, and Calibrated Value for the SWAT model's simulations of Furuna, Leliso, and Wabe river.

<b>Parameter Name</b>	<b>Description</b>	<b>Sensitivity rank</b>	<b>Calibrated range</b>	<b>Calibrated value</b>
SOL_AWC(..).sol	Available water capacity of soil layer	21	0-0.125	0.013
TLAPS.sub	Temperature lapse rate	20	4.50-10.00	6.353
GW_REVAP.gw	Groundwater 'revap' coefficient.	19	0.03-0.15	0.124806
SMFMN.bsn	Minimum snow melt rate during the year	18	5.43-17.01	10.749684
RCHRG_DP.gw	aquifer percolation fraction	17	0.27-0.74	0.319176
PLAPS.sub	Precipitation lapse rate	16	-275-315	-116.059
CH_N2.rte	Manning's "n" value for the main channel	15	0.015-0.235	0.1730
ALPHA_BNK.rte	Baseflow alpha factor for bank storage.	14	0.34-0.93	0.797
CH_L1.sub	Longest tributary channel length in sub basin	13	3.50-6.57	4.928
GWQMN.gw	Threshold depth of water in the shallow aquifer required for return flow	12	328-673	529.940
ALPHA_BF.gw	Baseflow alpha factor (days)	11	0.2-0.65	0.510477
SOL_Z(..).sol	Depth from soil surface to bottom of layer	10	721-1350	1157.661
CH_K1.sub	Effective hydraulic conductivity in tributary channel alluvium [mm/hr]	9	21-117	70.378
CN2.mgt	SCS runoff curve number.	8	37.5-71	43.891

GW_DELAY.gw	Groundwater delay (days)	7	147-215	187.199
REVAPMN.gw	Threshold depth of water in the shallow aquifer for "revap" (mm)	6	314-395	344.797
SOL_BD(..).sol	Moist bulk density	5	1-2.27	1.097
SNOCOVMX.bs n	Minimum snow water content	4	20-271	50.27942 7
SURLAG.bsn	Surface runoff lag time	3	18.5- 25.30	23.335
CH_K2.rte	Effective hydraulic conductivity in main channel alluvium.	2	375-470	418.535
SOL_K (...).sol	Saturated hydraulic conductivity	1	300-475	413.543

The sensitivity of flow parameters is presented in Table 4.3 and Figure 4.4, where SURLAG (Surface runoff lag time) is identified as the most sensitive parameter, while PLAPS (Precipitation lapse rate) is ranked as the least sensitive parameter.

#### **4.7 Model calibration and validation**

The model is calibrated and validated at the sub-basin level using monthly observed river discharge data. The calibrations and validations were accomplished for 19 years (January, 2000 to December, 2018) using streamflow measured at the three gauging stations within the Upper Wabe Shebele watershed. The calibration was performed for the first 12 years and the remaining 7 years data were used to validate the model. Streamflow data recorded at the Furuna, Leliso, and Wabe river gauging station were used to calibrate and validate the SWAT model. The calibration and validation processes involved the careful execution of semi-automated SUFI-2 (Sequential Uncertainty Fitting Version 2) within the SWAT-CUP framework, precisely conducted at monthly intervals. These procedures connected the power of the global sensitivity analysis method embedded in the SUFI-2 algorithm, enabling a comprehensive evaluation of model performance and accuracy across various scenarios and parameters. A total of twenty-one sensitive parameters were chosen. These parameters were refined by comparing modeled and observed flow data. The definitions, sensitivity rank, minimum and maximum values, as well as the calibrated values, are presented in (Table 4.3).

The calibration and validation performance were evaluated using three frequently used indicators: coefficient of determination ( $R^2$ ), Nash–Sutcliffe coefficient of efficiency (NSE), and percentage bias (PBIAS) (Moriasi et al., 2007). The concept of  $R^2$  is straightforward and widely understood; it indicates whether there is a linear relationship between observed and simulated data. The value typically ranges from 0 to 1, with values closer to one indicating a better fit (Santhi et al., 2002).

$$R^2 = \frac{\sum_{i=1}^n (O - O_m) * (S - S_m)}{\sqrt{\sum_{i=1}^n (O - O_m)^2 * \sum_{i=1}^n (S - S_m)^2}} \dots \dots \dots (6)$$

In the given context, the following variables are defined:  $R^2$  represents the coefficient of determination,  $O$  denotes the observed flow,  $O_m$  represents the mean observed flow,  $S_i$  signifies the model simulated flow,  $S_m$  represents the mean of the model simulations, and  $n$  denotes the total number of observations.

The Nash-Sutcliffe Efficiency (NSE) is a measurement used to assess the relative magnitude of the residual variance in comparison to the variance in the measured data. It provides a quantitative measure of the model's ability to reproduce the observed data (Cuceloglu et al., 2017). The calculation of NSE involves comparing the squared differences between the observed and simulated values with the squared differences between the observed values and their mean. By examining the relative variance, NSE allows for an evaluation of how well the model captures the variability and patterns present in the measured data (Moriasi et al., 2007; Santhi et al., 2002).

$$NSE = \frac{\sum_{i=1}^n (O - O_m)^2}{\sum_{i=1}^n (S - S_m)^2} \dots \dots \dots (7)$$

In this context,  $S$  represents the model simulated flow,  $O$  represents the observed flow,  $O_m$  represents the mean of the observations used as a benchmark for NSE,  $S_m$  represents the mean of the model simulations, and  $n$  represents the total number of observations indicating the goodness of fit between observed and simulated data.

$$PBIAS = 100 * \frac{\sum_{i=1}^n (S_m - O_s) i}{\sum_{i=1}^n Q_{m,i}} \dots \dots \dots (8)$$

In this context,  $Q$  represents the discharge,  $S_m$  and  $O_s$  stands for the measured and simulated values, respectively;  $n$  represents the total number of observations. **PBIAS** (Percent bias) measures the average tendency of the simulated flow to be either larger or smaller than the measured flow. Lower values indicate model overestimation, while higher values indicate model underestimation (Moriassi et al., 2007).

#### 4.8 Materials Used

For this research work, the materials utilized and their purpose are described in the Table 4.4.

Table 4.4 Different software's used and their purpose

<b>No</b>	<b>Software</b>	<b>Purpose</b>
<b>1</b>	ArcSWAT 2012.10_8.21	To delineate watershed, create HRUs, write weather input table, and Simulation the model.
<b>2</b>	ArcGIS 10.8	For creation thematic map and preparations of map layout.
<b>3</b>	SWAT_CUP	For sensitivity analysis, Calibrations and Validations of the model.
<b>4</b>	ERDAS IMAGINE 2015	For Land Use and Land Cover (LULC) Classification.
<b>5</b>	Surfer and Global Mapper 20.0	To create and prepare physiographic map.
<b>6</b>	Microsoft Excel	To organize climate data for model input.
<b>7</b>	Google Earth pro	To Supervise LULC Classifications.

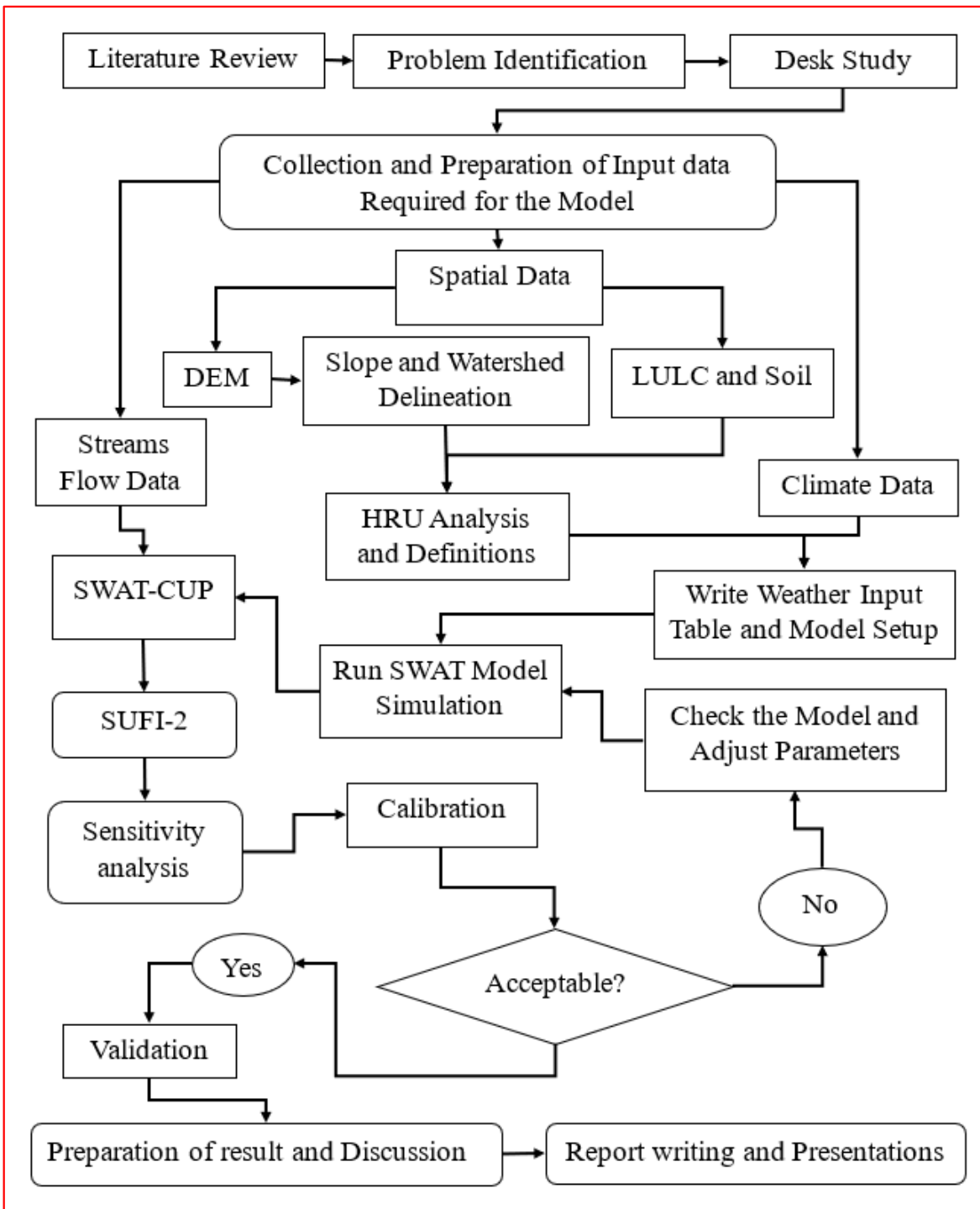


Figure 4.5 Flowchart of the Research Methodology.

## CHAPTER FIVE

### 5. RESULT AND DISCUSSION

#### 5.1 Annual water balance

A spatially distributed hydrological model was used to evaluate the major water balance components of the Upper Wabe Shebelle river basin, with particular emphasis on groundwater recharge estimation. The mean annual water balance components such as precipitation (PCP), actual evapotranspiration (AET), surface runoff (SURQ), recharge (RCHG) and baseflow (GWQ) were carefully extracted from the comprehensive simulation period of the SWAT model, precisely examined by harmonizing data from both the calibration and validation phases in order to provide the overall picture of the water balance of the basin. The long-term mean annual water budget components of the study area aggregated from daily modeling results over the whole simulation period (2000-2018) are displayed on Figure 5.1. The simulated water budget of the entire watershed showed that about 57.19% of the mean annual PCP that occurs in the watershed was lost through AET. The remaining portion is distributed among surface runoff (18.95%), groundwater recharge (22.33%), and a minor 1.53% allocated to baseflow (Table 5.1). This detailed analysis underscores the dominance of evapotranspiration as a pivotal process within the water balance components of the catchment.

Table 5.1 Annual water balance of the Upper Wabe Shebelle Basin (UWSB)

	A (km <sup>2</sup> )	PCP (mm)	AET (%)	RCHG (%)	SURQ (%)	GWQ (%)
<b>UWSB</b>	4413	961	57.19	22.33	18.95	1.53

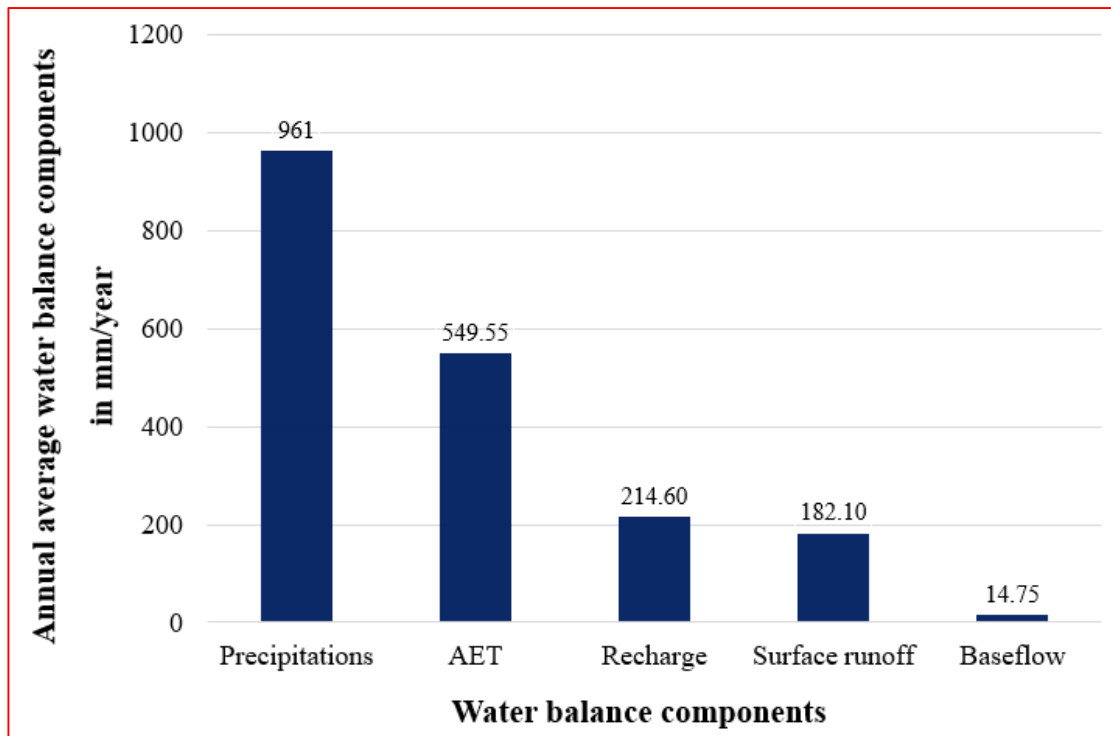


Figure 5.1 The average water balance components for the entire simulation period (2000-2018) of the Upper Wabe Shebele river basin.

## 5.2 Spatial distribution of Precipitation, Surface runoff, and Evapotranspiration

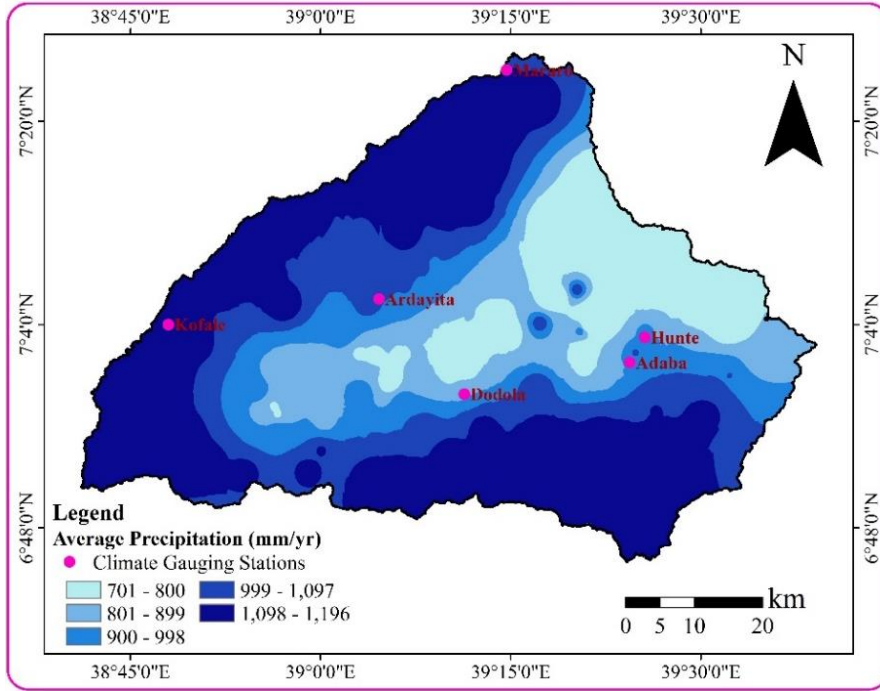
To gain a comprehensive understanding of how groundwater recharge is dispersed across a given area, it is beneficial to conduct an analysis of the spatial distribution of key factors that precede groundwater recharge: precipitation, surface runoff, and evapotranspiration. Precipitation holds significant importance as it serves as a fundamental driver for various hydrological processes. However, it also introduces a substantial degree of uncertainty when studying hydrological responses due to its inherent variability. The spatial distribution of precipitation plays a crucial role in shaping the spatial patterns and variations of other components within the water balance, such as surface runoff, and evapotranspiration. By examining the spatial distribution of these variables, valuable insights can be gained into the overall spatial patterns of groundwater recharge, thereby enhancing understanding of the hydrological dynamics within the studied area. Within the Upper Wabe Shebele catchment,

precipitation displays notable spatial variability, spanning from 701 mm/year (lowest) to 1,196 mm/year (highest). The central parts of the catchment experience the lowest precipitation values, while the western plateau, northern and southern highlands situated at the catchment's boundaries, observe the highest precipitation values. Figure 5.2 (A) illustrates that increase in precipitation from the central towards the Southern highland, Northern highland, and Western plateau. The relationship between precipitation and topography in the catchment is positive, indicating that topography influences the spatial variability of precipitation in the Upper Wabe Shebele Catchment.

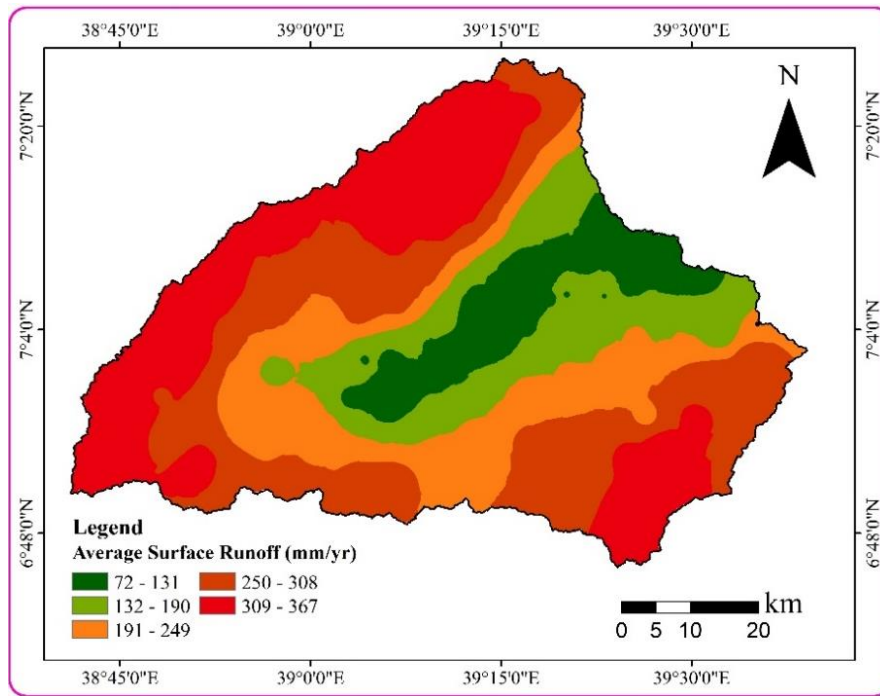
In the study area surface runoff is influenced by several factors, including precipitation amount and intensity, soil, LULC, and topography. Figure 5.2 (B) presents the long-term spatial distribution of mean annual surface runoff over an 18-year period (Jan-2000 to Dec-2018). Among the different regions within the current study area northern highland and western plateau exhibit the highest surface runoff, recording a value of 367mm/year. On the other hand, the central part of the catchment experiences the lowest runoff 72mm/year (Figure 5.2 B). This highlights a distinct spatial pattern where surface runoff increases progressively from the central plain of the catchment towards the northern highland, and western plateau. The variation in surface runoff within the study area can be explained by the distinct characteristics of the northern and southern catchment areas, as well as the central plateau. The northern and southern catchment areas exhibit steep topography, which facilitates the generation of runoff. In contrast, the central section of the study area consists of flat land, leading to lower levels of runoff generation. The relationship between vegetation and LULC significantly affect surface runoff. Vegetated areas generally experience lower surface runoff compared to non-vegetated surfaces under similar conditions. In the Upper Wabe Shebele watershed, above two-third of the catchment is covered by shallow-rooted agricultural plantations. These types of plantations exert minimal influence on the water balance compared to other LULC types. The southern part of the Upper Wabe Shebele watershed is distinguished for its vegetation cover (Figure 3.1). Although the area is covered with vegetation, this region experiences higher surface runoff despite receiving significant precipitation and having steep slopes. The steep topography significantly contributes to the increased surface runoff in this part of the catchment.

The permeability of subsurface and surface materials can significantly influence runoff processes. Runoff is more likely to occur in areas that have fine-grained, lower-permeability soils as opposed to areas of coarse-grained, higher-permeability soils. In the Upper Wabe Shebele watershed, rainfall variability has a predominant impact on surface runoff, while soil variability contributes to spatial distribution to a lesser degree. The central region of the Upper Wabe Shebele Catchment is largely covered by cambisols, as classified by the FAO (Figure 4.2). This soil type, prevalent across the Gedeb-Asasa plain, is typically well-drained and varies from moderately deep to very deep, with textures ranging from fine to medium clay loam and sandy loam. As a result, small amounts of surface runoff can occur in this area, where precipitation occurred in the region often lost by soil infiltration and evapotranspiration. Additionally, a large portion of the basin is covered by Vertisols and Luvisols, while a smaller area shielded by humic Nitisols. However, their influence on the spatial variability of surface runoff has not been significantly recognized. Instead, LULC, land-surface topography and rainfall amounts play a dominant role in determining surface runoff within the catchment area. Steep slopes tend to result in higher runoff rates. A comparison of the surface runoff map (Figure 5.2 B) with the physiography of the study area (Figure 3.4) clearly highlights the significant impact of topography on runoff patterns for the area having the same land use land cover.

The Upper Wabe Shebele Catchment exhibits variable evapotranspiration rates (Figure 5.2 C). A large region of the watershed has evapotranspiration levels ranging from 343mm/year to 606mm/year. To estimate evapotranspiration, the model uses the Hargreave method, which takes into account the highest and lowest temperatures of each day, along with the amount of precipitation. As a result, areas with high temperatures and low rainfall, have higher evapotranspiration values. The LULC map (Figure 4.1) shows that a water body is located in the eastern central part of the watershed, where evaporation rates are high. Additionally, the LULC map indicates that mixed forest plants are located in the southern highlands of the watershed. In this region, evapotranspiration's rates are higher compared to areas receiving similar amounts of rainfall. Variations in precipitation and temperature significantly impact the spatial distribution of actual evapotranspiration across the basin. The lowest levels of evapotranspiration are simulated in highland areas, primarily due to the region's minimum temperatures and steep topography.



A)



B)

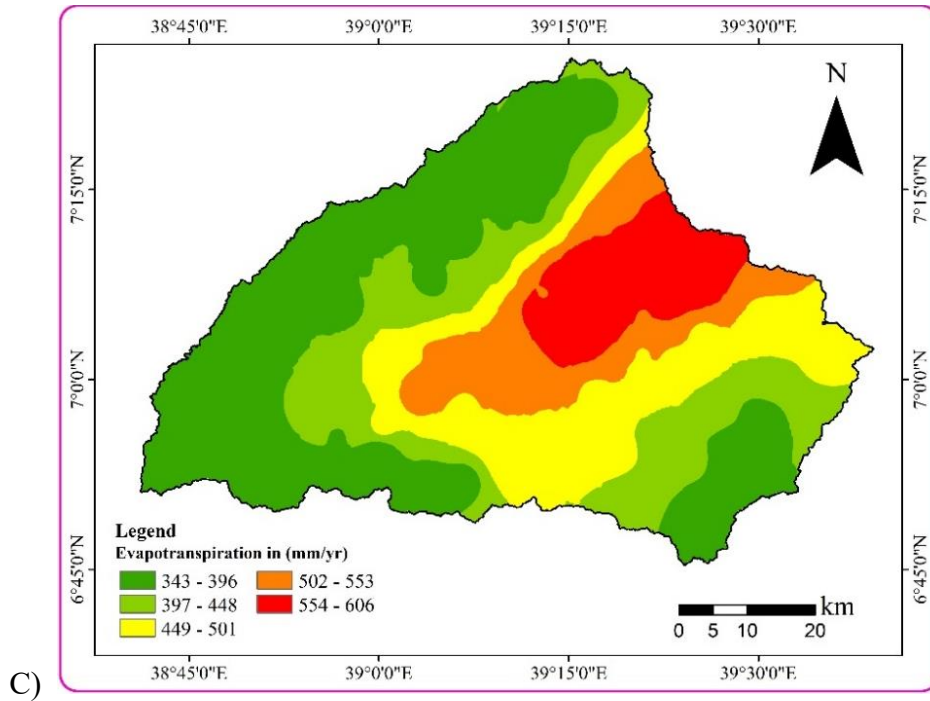


Figure 5.2 The long term (2000-2018) annual spatial distribution of water balance components: A) Precipitation, B) Surface Runoff. and C) Evapotranspiration.

## 5.3 Groundwater Recharge

### 5.3.1 Spatial groundwater recharge variability

Recharge rates can vary considerably across different locations within a given area. The Soil and Water Assessment Tool (SWAT) model was used to estimate the long-term mean annual groundwater recharge for the entire watershed. According to the SWAT model results, the estimated long-term mean annual groundwater recharge for the entire watershed is approximately 214.7mm/year (Figure 5.1). This suggests that the watershed experiences a significant amount of groundwater replenishment on an annual basis, which is an important watershed water balance component. However, relying solely on a single average recharge rate for an entire area would oversimplify the complex nature of groundwater recharge and may lead to inaccurate assessments. To obtain a more accurate and reasonable understanding of recharge patterns, it is crucial to consider and analyze the spatial variations in groundwater recharge.

The study approach involves examining groundwater recharge rates at specific locations within the study area. These recharge rates are influenced by a variety of factors, including the local hydrogeological conditions, land use practices, and climate variations. The local hydrogeological conditions, such as soil permeability and the presence of geological formations, can greatly impact the rates of groundwater recharge. Additionally, land use activities like urban development and agriculture can affect the amount and timing of recharge. Climate factors, such as rainfall patterns, rainfall intensity, and evapotranspiration rates, play a dominant role in the groundwater recharge process. Analysis of the spatial distribution shown on (Figure 5.3) reveals a significant variation in groundwater recharge across the study area. There is a consistent pattern of increasing recharge rates from the central plain toward the western plateau, northern highlands, and southern highlands. In the central plain areas of the basin, the average recharge is approximately 101mm/year. However, as it moves from the central plain towards the highland regions, the average recharge progressively rises to 315mm/year. This significant variation in groundwater recharge is observed, with notably higher rates in the highland regions compared to the lowland areas of the basin. This difference is attributed to the catchment's diverse climate. Moving from the central plain toward the western plateau, southern highland, and northern highland, temperatures gradually decrease while both the amount and intensity of precipitation increase.

Variations in groundwater recharge across the study area are influenced by factors like rainfall intensity, topography, geology, and LULC. In the central and northeastern parts of the upper Wabe Shebele catchment, groundwater recharge is notably low. This phenomenon can be attributed primarily due to the region's high temperatures, which lead to increased evaporation rates. The combination of high temperatures and low precipitation creates a challenging environment for water holding in the soil. Land-surface topography plays a crucial role in both diffuse and focused groundwater recharge processes. A comparison of the spatial rainfall map (Figure 5.2A) with the physiographic map of the study area (Figure 3.4) reveals a direct relationship between the amount of precipitation and the region's topography. Especially, the WPLT, SHL, and NHL areas receive the highest levels of precipitation, which enhances groundwater recharge in these regions.

However, in the southern part around the summit of the Bale Mountains and the northern part near the Honkolo Shield Volcanoes, groundwater recharge is lower than the surrounding regions having similar precipitation levels (Figure 5.4). This inconsistency highlights that the significant influence of topography on groundwater recharge, despite the high rainfall in these areas. Vegetation and LULC are vital for groundwater recharge. In the Upper Wabe Shebele watershed, about 68.46% of the area is agricultural land (Figure 3.1). The depth of plant roots affects water extraction; larger plants can access moisture at several meters, while shallow-rooted crops can only reach the upper soil layers. Although agricultural land dominates the basin, its impact on water balance is limited compared to other land cover types. Vegetation influences recharge seasonally; during periods of decay, plants can enhance recharge by exposing cavities that act as preferential flow channels. At the eastern central part of the Upper Wabe Shebele catchment, there is an open water body (Malka Wakana Hydroelectric Power) where groundwater recharge is assumed to be negligible. Generally, while the impact of LULC has been observed in the study area, it is not as significant as the influence of climate.

The permeability of surface and subsurface geological materials significantly affects groundwater recharge processes. Recharge is more likely to occur in areas with coarse-grained, highly permeable geological materials compared to regions with fine-grained, less permeable materials. In the Upper Wabe Shebele River Basin, while the influence of variable geological materials on groundwater recharge is not as pronounced as that of climate variability, it does contribute modestly to the spatial variability of groundwater recharge. Permeable geological materials possess a relatively high capacity for rapidly transmitting water. In the western, northern, and southwestern regions of the Upper Wabe Shebele Catchment, the higher density of lineaments promotes greater groundwater recharge.

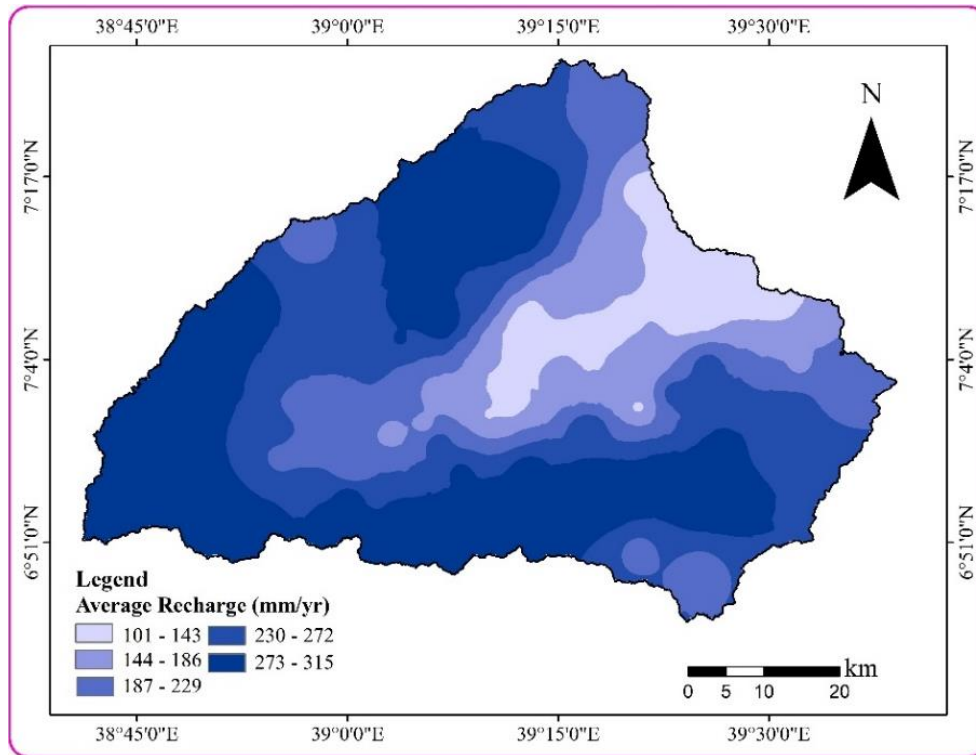


Figure 5.3 Spatial groundwater recharge map of the Upper Wabe Shebele Basin.

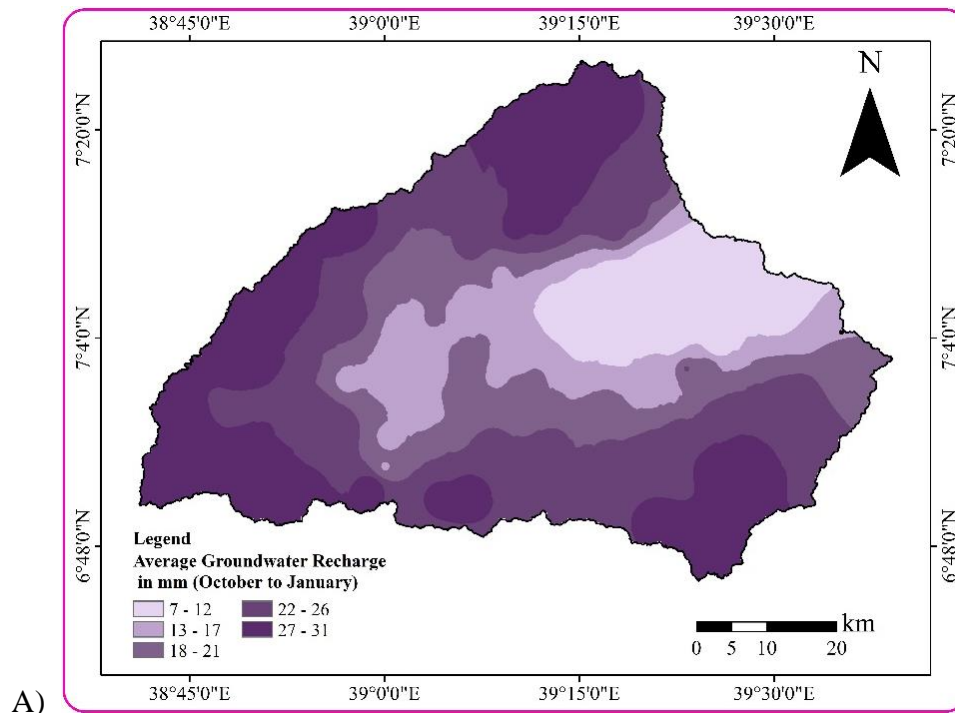
### 5.3.2 Temporal groundwater recharge variability

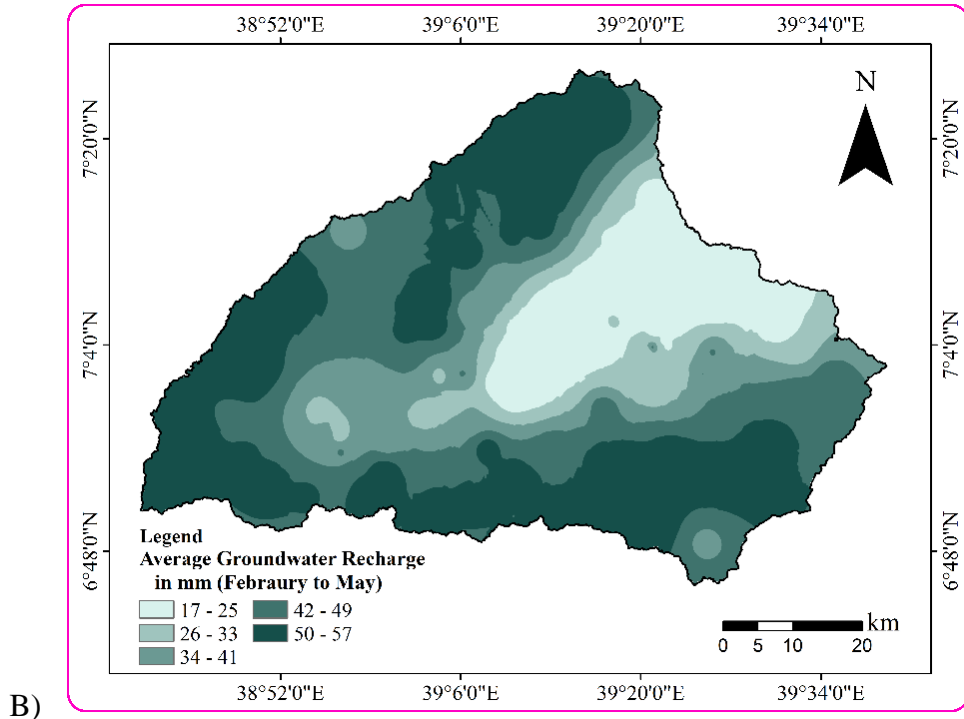
The findings from the SWAT model analysis have provided valuable insights into the groundwater recharge patterns within the Upper Wabe Shebele catchment. The results indicate that groundwater recharge exhibits variations both within a single year (intra-annually) and between different years (inter-annually). On an intra-annual basis, the groundwater recharge levels fluctuate throughout the seasons. Factors such as rainfall patterns, evapotranspiration rates, and soil moisture content contribute to these variations. During the wet season, characterized by higher precipitation and lower evapotranspiration, groundwater recharge tends to be more substantial. In contrast, the dry season, with reduced rainfall and higher evapotranspiration, leads to lower groundwater recharge levels. Furthermore, the inter-annual analysis reveals that groundwater recharge varies from year to year within the Upper Wabe Shebele catchment. This variability can be attributed to factors such as annual rainfall variations, changes in land use and land cover, and climate fluctuations. Some years may experience higher

recharge rates due to above-average rainfall, while others may have lower recharge rates during periods of drought or reduced precipitation.

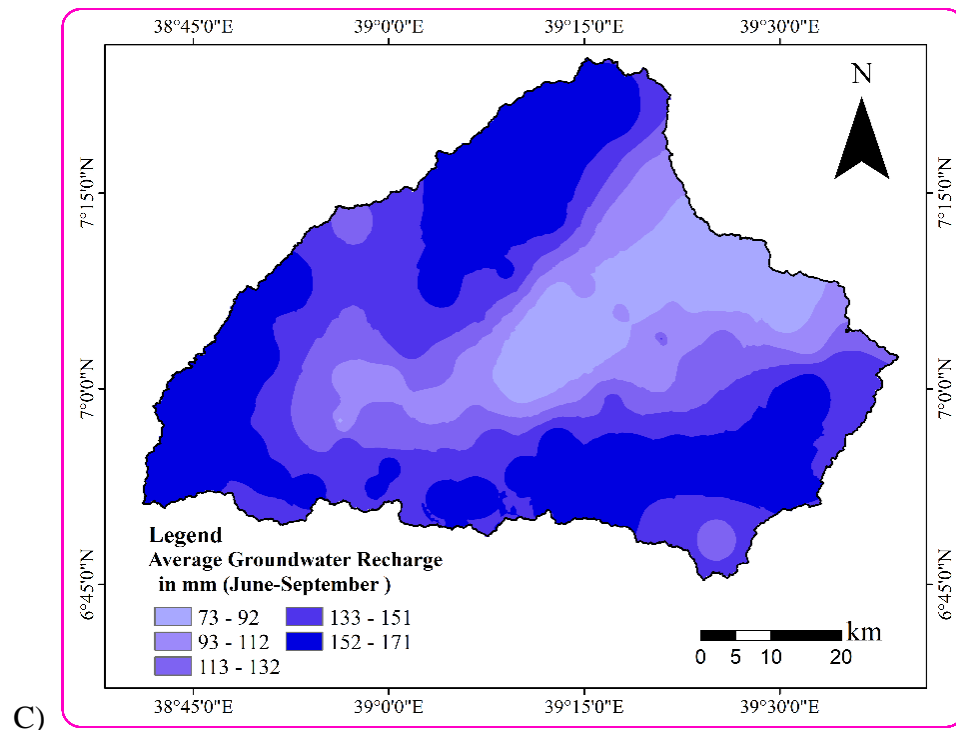
### 5.3.2.1 Intra-annual groundwater recharge variability

In Ethiopia, the classification of seasons is determined by the precipitation patterns. According to the National Meteorological Services Agency (NMSA) in 1996, Ethiopia experiences three main seasons: Kiremt, Belg, and Bega. The Kiremt season, which occurs from June to September, is considered the primary rainy season in Ethiopia. The Belg season, on the other hand, is a smaller rainy season that typically takes place from February to May. Finally, the Bega season is the dry season observed from October to January. This classification of seasons is generally applicable to most parts of Ethiopia, particularly in the northern, northeastern, southeastern, central, and western regions. It provides a framework for understanding and predicting the rainfall patterns in these areas.





B)



C)

Figure 5.4 Spatial variability of groundwater recharge within year from season to season. (A) October-January (Bega season), (B) February-May (Belg season) and (C) June-September (Kiremt).

In order to obtain a detail understanding of temporal groundwater recharge, the basin was divided into four distinct physiographic regions, namely the Western Plateau (WPLT), Central plateau (CPLT), Southern highland (SHL), and Northern highland (NHL). This subdivision took into consideration the hydrologic characteristics of the area. Based on the analysis of the average monthly precipitation graph Figure 5.5 (A), it is evident that the catchment area exhibits a nearly bimodal precipitation pattern. This means that there are two distinct seasons in precipitation occurring at different times throughout the year. Such a bimodal pattern suggests that the area experiences two main periods of increased rainfall. Furthermore, the examination of average monthly groundwater recharge in relation to precipitation reveals a positive correlation. This implies that as precipitation levels increase, there is a corresponding rise in groundwater recharge within the catchment. The positive correlation indicates that the amount of groundwater replenishment is influenced by the amount of rainfall received during a given month. Higher precipitation leads to increased groundwater recharge, contributing to the overall water availability and storage in the catchment area.

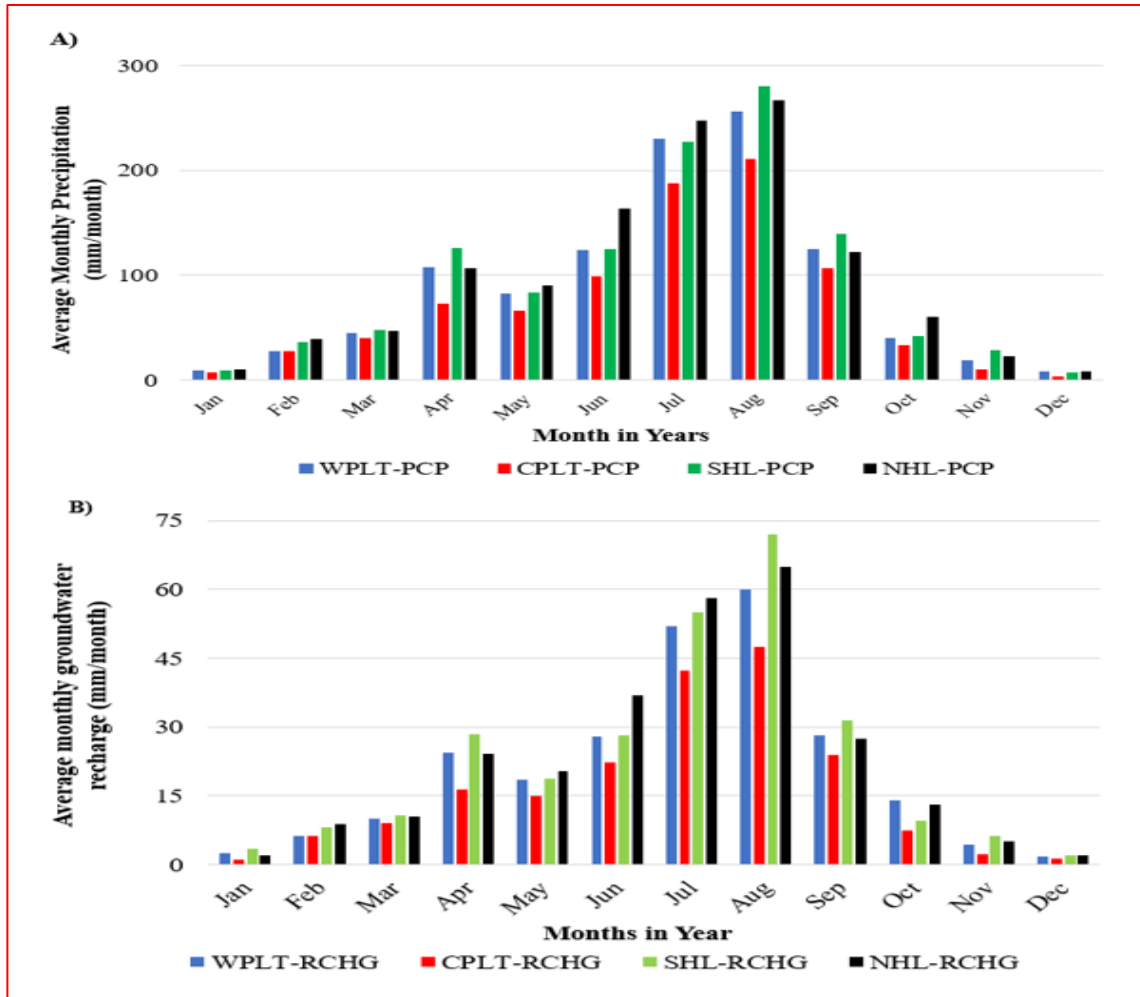


Figure 5.5 Average monthly groundwater recharge with compared to average monthly precipitation at different physiographic regions (mm/month) within the study area. A) WPLT, CPLT, SHL, and NHL Average monthly precipitations (mm/month), and B) WPLT, CPLT, SHL and NHL groundwater recharge (mm/year).

### 5.3.1.2 Inter-annual groundwater recharge variability

The year-to-year variability of groundwater recharge in the Wabe-Shebele river basin is primarily influenced by the temporal distribution of precipitation, as depicted in (Figure 5.6). The correlation between annual average precipitation and groundwater recharge values (inter-annual correlation) demonstrates a positive relationship, indicating that changes in precipitation directly affect groundwater recharge. (Figures 5.6A and 5.6B) illustrate this positive response, showing the correlation between annual average precipitation and groundwater recharge values

in the four physiographic regions of the upper Wabe-Shebele River Basin: Western Plateau (WPLT), Central Plateau (CPLT), Southern Highland (SHL), and Northern Highland (NHL). The data reveals that as precipitation increases, there is a corresponding increase in groundwater recharge for each specific region, and vice versa. This strong link between precipitation and groundwater recharge highlights the sensitivity of the groundwater system to changes in precipitation patterns.

Furthermore, the analysis of the graphical representations in (Figure 5.6) provides valuable insights into the relationship between precipitation, topography, land use/land cover, and groundwater recharge in the region. It clearly demonstrates that the western plateau, southern, and northern highlands of the Upper Wabe-Shebele river basin experience high levels of precipitation, and these areas also exhibit high rates of groundwater recharge. This observation suggests that as the intensity of precipitation increases, there is a corresponding rise in groundwater recharge in these regions. The strong positive correlation between precipitation and groundwater recharge, as well as the spatial distribution of these variables, underscores the importance of considering the relationship between climatic factors, topography, geology, and land use/land cover when assessing and managing the groundwater resources in the Upper Wabe-Shebele river basin. The interplay between the physical characteristics of the terrain and the vegetation cover carried out on the land surface plays a crucial role in shaping the availability and replenishment of groundwater. The steep topography of the highland areas likely influences the movement and distribution of water, affecting the rate at which it percolates through the soil and replenishes underground aquifers.

Additionally, land use and land cover, such as, urban development and vegetation cover can significantly alter the hydrological processes. These can lead to increased surface runoff, reduced infiltration, and ultimately lower groundwater recharge rates. By considering the inter-annual correlation and the influence of precipitation, topography and land use/land cover on groundwater recharge, water resource managers and planners can make informed decisions regarding sustainable water management practices. This knowledge enables the development of strategies that account for the inconsistency of these factor and their impact on groundwater recharge in order to ensure the efficient and responsible use of the resource.

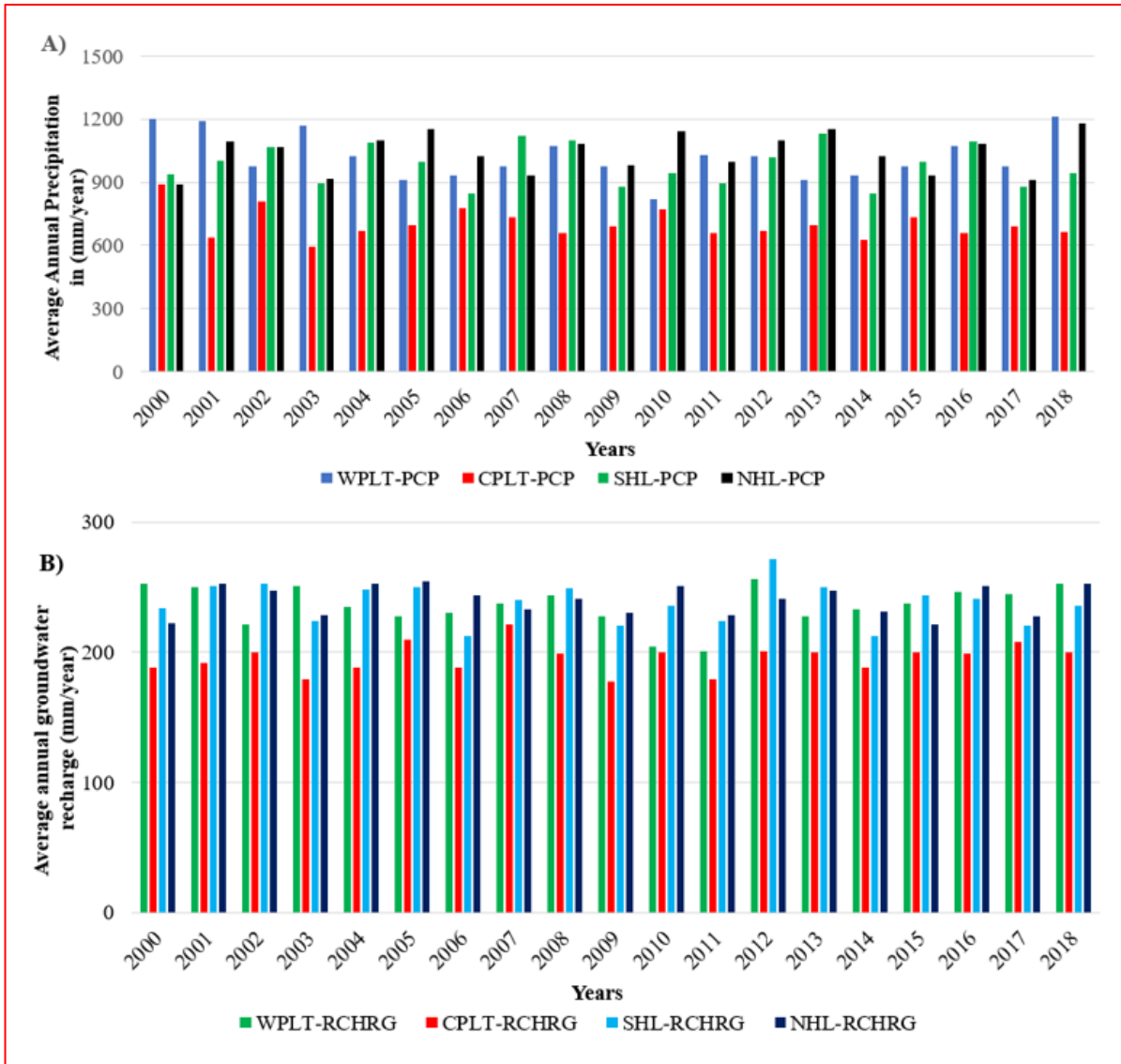


Figure 5.6 Average annual groundwater recharge with compared to average annual precipitation at different physiographic regions. A) WPLT, CPLT, SHL, NHL precipitation (mm/year), B) WPLT, CPLT, SHL, NHL groundwater recharge (mm/year).

## **5.4 Governing factors for variability of groundwater recharge**

The hydrology of a basin can be influenced by various factors, including climate, geology, topography, vegetation, and land use/land cover (LULC). Climate, particularly precipitation and temperature, plays a significant role in determining the groundwater recharge within a watershed. Precipitation serves as the primary source of natural groundwater replenishment and is a dominant component in the water budget of the basin. The temporal variability of precipitation, including seasonal patterns, inter-annual variations, and long-term trends, as well as the intensity of precipitation events, greatly impact the processes involved in groundwater recharge within the Upper Wabe Shebele basin. The fluctuations in precipitation patterns can have primary effects on the groundwater recharge dynamics within the basin. Changes in the amount and distribution of rainfall directly influence the availability of water for recharge. Variations in precipitation, both in terms of timing and intensity, can significantly affect the recharge processes occurring in the Upper Wabe Shebele basin. It is important to consider the interplay of these climatic factors with other elements such as soil, geology, topography, vegetation, and LULC when assessing the overall hydrological behavior of the basin. Understanding the complex interactions among these factors is crucial for effectively managing and sustaining water resources in this basin.

The spatial distribution of precipitation and temperature, along with their temporal variability, significantly influences groundwater recharge within the Upper Wabe Shebele basin. Upon examining the groundwater recharge map (Figure 5.3), it becomes clear that the western plateau, as well as the northern and southern highlands of the basin, are the most rechargeable zones. This distinction arises due to the high levels of precipitation in the highland areas and high lineament density of these regions. The uneven distribution of topography and geological materials across the watershed explains this disparity, leading to varying recharge patterns. Identifying these specific regions enhances our understanding of the spatial dynamics of groundwater recharge in the basin, crucial for effective water resource management and planning. This knowledge enables the implementation of targeted strategies in areas with high recharge potential, promoting sustainable use of groundwater resources within the catchment. The catchment exhibits seasonal trends in evapotranspiration rates, with the highest rates occurring during dry months and the lowest rates during rainy months. This indicates that

evapotranspiration is influenced by the availability of water and follows a pattern aligned with the precipitation patterns. The study of the spatial and temporal variability of groundwater recharge in the region has revealed the significant influence of precipitation on recharge processes. Both the temporal and spatial variability of precipitation play crucial roles in determining the groundwater recharge dynamics within the basin.

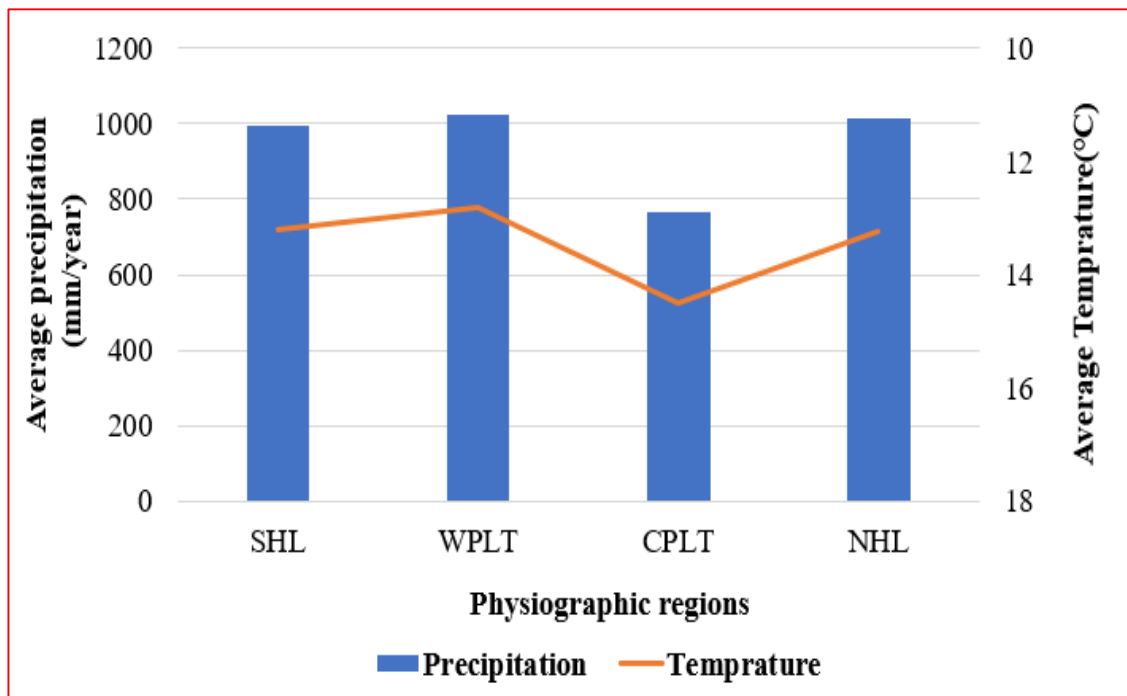


Figure 5.7 Average annual variation in climate (precipitation and temperature) across various physiographic regions of Upper Wabe Shebele river basin.

The permeability of geologic materials is a critical factor in groundwater recharge processes. Areas with coarse-grained, high-permeable materials have a higher likelihood of groundwater recharge compared to areas with fine-grained, low-permeable materials. The high permeability of coarse-grained geologic materials enables water to flow more rapidly through them. In the Upper Wabe Shebele basin, the variability of geologic materials has a significant influence on groundwater recharge. It plays a crucial role in determining the spatial variability of groundwater recharge within the region. The properties of geologic materials, including permeability and porosity, have direct implications for the rate and extent of groundwater replenishment. By considering the variability of geologic materials, measures can be taken to

optimize groundwater recharge and sustainably utilize the available water resources in the region. The interplay between geological formations and topographical features has a noticeable impact on groundwater replenishment in the peripheral part of northeastern and southeastern highlands situated in the Upper Wabe Shebele basin.

Consequently, the peripheries of the northeastern, southern, and southeastern highlands experience relatively reduced rates of groundwater recharge compared to the surrounding regions, despite being areas with higher rainfall levels. This highlights the crucial importance of carefully considering the effects of geological materials and topography when analyzing the complex dynamics of groundwater recharge in a catchment area. The spatial and temporal variability of groundwater recharge in the Upper Wabe Shebele basin is governed by several factors, including climate conditions, land use and land cover (LULC), soil properties, and slope phenomena. These factors collectively influence the recharge patterns within the basin. The SWAT model has been employed to simulate groundwater recharge values, revealing distinct spatial variations. The central part of the basin, characterized by low-lying areas, exhibits lower simulated groundwater recharge values compared to the western plateau, northern and southern highlands. The findings highlight the significance of climate as the most influential factors contributing to the spatial and temporal variability of groundwater recharge in the Upper Wabe Shebele basin. These factors interact and shape the recharge dynamics in the region.

## 5.5 Model performance evaluation

Statistical methods were used to measure SWAT performance, aiming to verify the reliability and precision of its simulations against real data. SWAT-CUP was employed to assess the model's streamflow simulation capability using criteria like  $R^2$ , NSE, and PBIAS. In this study, the SWAT model was simulated using climate data (daily precipitation, daily maximum and minimum air temperatures, daily relative humidity, daily wind speed, and daily solar radiation) from January, 1998 to December, 2018 covering a period of 21 years. Streamflow data of three gauging stations from, 1998 to 2018 was used for SWAT model warmup, calibration, and validation purposes. The calibration was performed on a monthly basis downstream of the gauging stations for Furuna, Leliso, and Wabe rivers (Figure 5.8). To warmup, calibrate and validate its performance, flow data from these rivers were utilized for different time periods. Specifically, data from 1998 to 1999, 2000 to 2011, and 2012 to 2018 were used for warmup, calibration, and validation, respectively. The model was calibrated manually by adjusting the most sensitive parameters determined from the sensitivity analysis to obtain the best fit between simulated and observed flow data. Even though this calibration step was tedious and time consuming, the obtained result is quite interesting. The Sequential Uncertainty Fitting Program (SUFI-2) of SWAT-CUP package was employed for parameter optimization to achieve the optimal alignment between the simulated data and observed data. In order to optimize the performance of the model, the parameters were subjected to a range of values within predefined bounds.

This allowed for the exploration of different parameter combinations and adjustments, leading to the determination of the optimal parameter values or relative changes for spatially varying parameters. The goodness of fit tests like, Coefficient of Determination ( $R^2$ ), Nash and Sutcliffe Efficiency Criteria (NSE) and PBIAS which were used to evaluate the model performance on monthly basis have showed a good agreement (Table 5.21). The goodness of fit is comprehensive above the recommended minimum values of ( $R^2 > 0.60$ ,  $NSE > 0.50$  and  $(-15 < PBIAS \leq +15)$ ) (Moriasi et al., 2007; Santhi et al., 2002; Trivedi et al., 2023).

The Coefficient of Determination ( $R^2$ ) for Furuna river is 0.88 and 0.79; for Leliso river is 0.65 and 0.67, and for Wabe river is 0.88 & 0.66 during calibration and validation period respectively. Similarly, Nash-Sutcliffe Efficiency (NSE) value for Furuna river is 0.73 and 0.71; Leliso river

is 0.77 and 0.58, and for Wabe river is 0.70 and 0.71 during calibration and validation period respectively. Additionally, PBIAS value for Furuna river 5.73 and -11.35; for Leliso river 14.0 and 6.43; and for Wabe river 11.53 and -5.73 during calibration and validation period respectively. These result indicates that the goodness of fit test exceed the recommended minimum values and demonstrates a good model outcome as per (Moriasi et al., 2007; Santhi et al., 2002). Overall, the graphical visualizations of the simulated monthly stream flow against the observed stream flow during the calibration and validation periods were assessed (Figure 5.8 A, B, and C). The visual comparison of the observed and simulated hydrographs reveals closely matching rising and recession limbs, convincing that the model effectively captures seasonal variations. However, the relatively low correlation may be linked to the quality of the river flow data and input data, particularly the climate data, which had some missing values that were manually filled using an arithmetic mean method this could contribute to deviations. The calibrated SWAT model for the Upper Wabe Shebele river basin was also validated with the same parameters, without any further modifications to the model inputs. Finally, the calibration and validation results indicated that the SWAT model effectively simulated monthly river discharge. Thus, it can be concluded that the SWAT model developed for the upper Wabe Shebele river basin accurately reflects the hydrological flows in the basin and is suitable for upcoming impact studies.

Table 5.2 Goodness fit considered for model

Gauging station	Model stages	Objective function		
		R <sup>2</sup>	NSE	PBIAS
Furuna	Calibration (2000–2011)	0.88	0.73	5.73
	Validation (2012–2018)	0.79	0.63	-11.35
Leliso	Calibration (2000–2011)	0.65	0.77	14.0
	Validation (2012–2018)	0.67	0.58	6.43
Wabe	Calibration (2000–2011)	0.88	0.70	11.53
	Validation (2000–2018)	0.66	0.71	-5.13

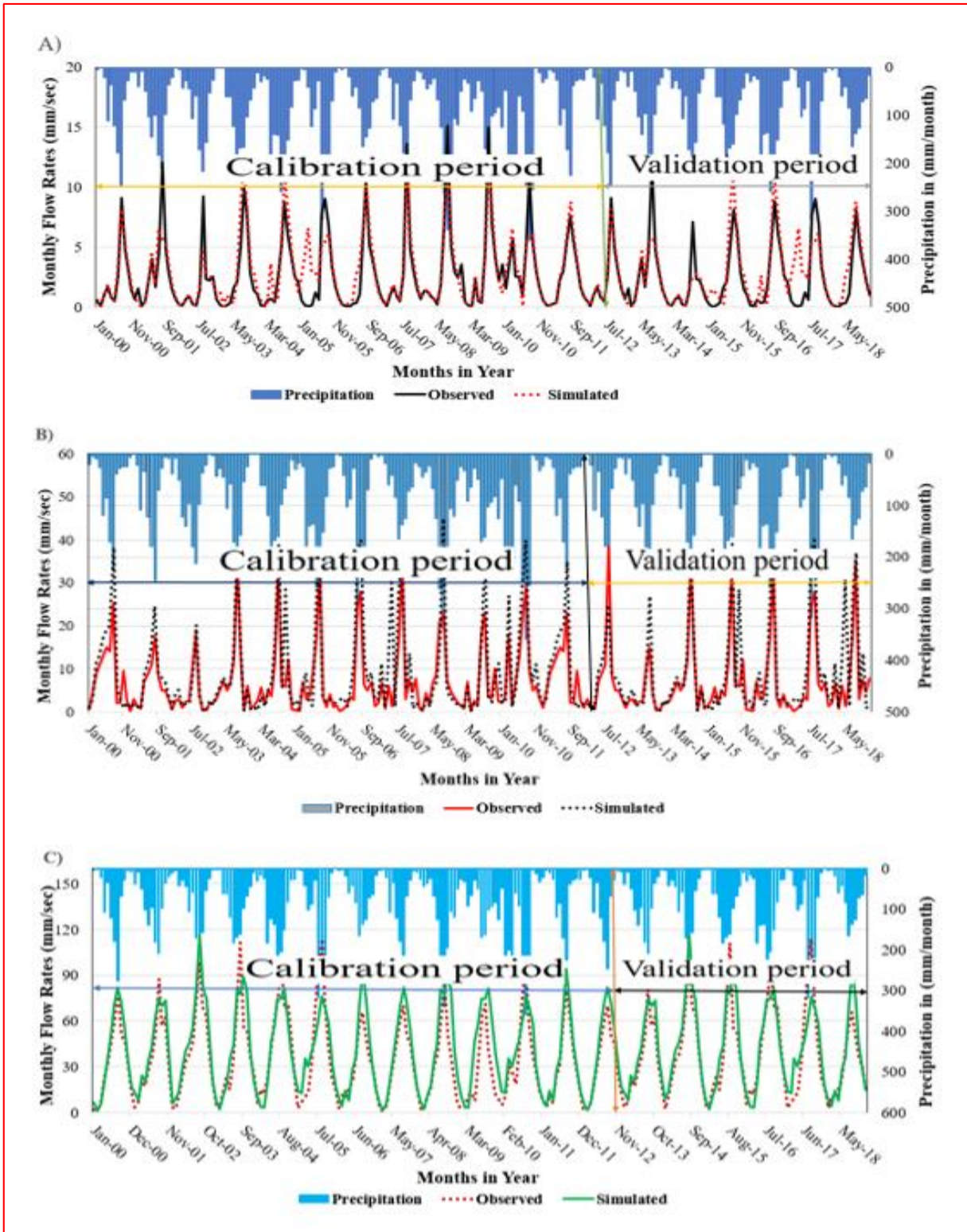


Figure 5.8 Monthly time series of measured and simulated average discharge of A) Furuna B) Leliso and C) Wabe River for the calibration (2000-2011) and validation (2012-2018) periods.

## CHAPTER SIX

### 6. CONCLUSIONS AND RECOMMENDATIONS

#### 6.1 Conclusion

The Upper Wabe Shebele Catchment in southeastern Ethiopia is considered a critical area for hydrological studies due to its unique climate, topography, and land use. This watershed is characterized by a bimodal rainfall pattern, a range of topographies from flat plains to steep slopes, and extensive agricultural land that makes up above two-thirds of its total area. Understanding groundwater recharge in this catchment is essential for sustainable water resource management, especially in regions facing water scarcity. In the present study, the physically based water budget model, SWAT have successfully been applied to estimate groundwater recharge by analyzing various water balance components. The model was set up to operate on a daily time step, but the results were aggregated to both monthly and yearly scales for analysis.

The Upper Wabe Shebele River basin is principally made up of Cenozoic volcanic rock. The Cenozoic volcanism in this study area includes records of flood basalts and bimodal basalt-rhyolite/trachyte-pyroclastic volcanism, which Extending from the Tertiary to the Quaternary period. The geological mapping of the study area entails that area constitutes nazreth group and dino formation, plateau basalt, upper pyroclasts, highland basalt flows, Alkali trachyte flows with some plugs, Trachytic tuffs with minor basalt and alkali trachyte flows and sediments, interlayered alkali trachyte and basalt flows, Pliocene basalt flows, Pliocene trachyte flows, and Quaternary alluvial deposits. The hydrogeological characteristics of the Wabe Shebele basin are shaped by various factors, including geological formations, structural conditions, geomorphology, and climate with two main contributors being the east-west and south east-north west mountain ranges that facilitate groundwater recharge through rainfall collection. The basin's aquifers are classified into five types based on porosity and permeability, ranging from highly productive fractured volcanic aquifers to low productive ones, each exhibiting varying discharge rates and characteristics. The extensive volcanic aquifer system, particularly within the Tertiary Volcanics, plays a crucial role in groundwater dynamics.

The long-term annual water balance analysis from 2000 to 2018 revealed that approximately 57.19% of the mean annual precipitation in the Upper Wabe Shebele Catchment is lost to evapotranspiration. The remaining precipitation is partitioned into surface runoff (18.95%), groundwater recharge (22.33%) and 1.53% allocated to baseflow. This finding highlights the significance of evapotranspiration as the primary consumer of precipitation in the area.

Groundwater recharge showed significant spatial and temporal variability during the simulation period. Average annual recharge decreased from 315 mm/year in the highlands to 101mm/year in the central plains, influenced by precipitation intensity, temperature, soil characteristics, and land use. Intra-annually, recharge was lower from October to January (Bega season) and higher from June to September (Kiremt season). Inter-annually, precipitation and groundwater recharge trends were consistent across all regions. The simulation results show a strong correlation between groundwater recharge and annual precipitation patterns, following a bimodal wet cycle. Various factors affect the spatial and temporal variability of groundwater recharge in the Upper Wabe Shebele Catchment. Precipitation is the primary driver, with increased rainfall boosting recharge rates in the summer. Land use and land cover (LULC) changes also impact infiltration rates and surface runoff, influencing recharge dynamics. Additionally, soil characteristics, including texture and permeability, are crucial for determining water infiltration and groundwater recharge. Furthermore, the catchment's topography, including elevation and slope, influences water flow patterns and distribution, thereby affecting recharge rates in various regions. The model was calibrated from 2000 to 2011 and validated from 2012 to 2018 using river discharge data collected from three gauging stations: Furuna, Leliso, and Wabe rivers. The model was manually calibrated by adjusting key sensitive parameters identified in the sensitivity analysis to improve the fit between simulated and observed flow data. The Sequential Uncertainty Fitting Program (SUFI-2) from the SWAT-CUP package was used for parameter optimization to enhance alignment between the simulated and observed data. The performance metrics during the calibration and validation phase were promising and showed acceptable ranges of model evaluation indicators ( $R^2 = 0.58-0.77$ , NSE = 0.65–0.81, PBIAS = 5.13–14.00). These metrics indicate that the model accurately simulates river discharge and can be used to estimate groundwater recharge for the upper Wabe Shebele watershed effectively.

The hydrological modeling of the Upper Wabe Shebele Catchment provides valuable insights into groundwater recharge processes, with the SWAT model effectively estimating recharge rates and demonstrating strong performance during calibration and validation phases. Understanding the spatial and temporal variability of groundwater recharge is essential for effective water resource management in the watershed.

## **6.2 Recommendation**

Based on the findings of the research, the successive key recommendations are proposed. Assessing groundwater recharge solely through a single indirect method like Potential Recharge poses challenges in ensuring reliability, despite detailed discussions on its spatial and temporal variability. It is therefore advisable to complement this approach by employing an alternative method, such as direct methods, to enable a comparative analysis with the estimates derived from the SWAT model. Based on the findings of this study, it can be deduced that the spatial and temporal fluctuations in groundwater recharge are significantly influenced by climate factors. Given this observation, it is strongly advised to evaluate the potential impacts of future climate change through the utilization of climate model projections. By incorporating these projections into assessments of groundwater recharge dynamics, a more comprehensive understanding of the evolving hydrological landscape can be attained, facilitating informed decision-making in water resource management and adaptation strategies. The geological structure plays a vital role in groundwater recharge, yet the SWAT model may not fully capture its impact. While the model offers estimates of potential groundwater recharge, these figures could be underestimated due to significant water access along geological lineaments. Therefore, it is essential to consider the influence of the geological structure on groundwater recharge within the basin in further investigations to achieve more accurate and realistic results. Integrating an understanding of the geological features and their effect on groundwater dynamics in related studies is crucial for enhancing the precision of groundwater recharge assessments.

## REFERENCES

- Abbaspour, K. C., Yang, J., Maximov, I., Siber, R., Bogner, K., Mieleitner, J., Zobrist, J., & Srinivasan, R. (2007). Modelling hydrology and water quality in the pre-alpine/alpine Thur watershed using SWAT. *Journal of Hydrology*, 333(2–4), 413–430. <https://doi.org/10.1016/j.jhydrol.2006.09.014>
- Adams, S., Titus, R. (Rian), Xu, Y. (Yongxin), & South Africa. Water Research Commission. (2004). *Groundwater recharge assessment of the basement aquifers of Central Namaqualand : report to the Water Research Commission (WRC)*.
- Agezew, T., Regassa, T., & Sima, J. (2014). *Hydrogeological and Hydrochemical Maps of Dila NB 37-6*.
- Alemayehu, G., Birhanu, Wondaferaw Getahun, S., Hambisa, G., Kifletsion, B., Kiros, M., Mandefro, B., Mesfin, A., Samson, T., Solomon, B., Tedesse, A., & Tesfaye, K. (1991). *Geological Map of Dodola Map Sheet*.
- Aman, Y., Bezayit, M., Berhanu, B., Tesfay, G., Terkegn, D., Yonas, T., Weynu, T., & Rahel, A. (2012). *Geological Map of Dila Map Sheet (NB37-6)*.
- Andy, D. W., & Stanley, W. T. (2003). *Environmental Hydrology* (Second Edi). Lewis.
- Arnold, J., Srinivasan, R., Muttiah, R., & Williams, J. R. (1998). Large area hydrologic modeling and assessment part I: model development. *Journal of the American Water Resources Association* , 34(1), 73–89.
- Astatike Kiflu, & H/Mariam, M. (2010). *Integrated Hydrogeological Mapping of Dodola Map Sheet (NB 37-7) South Eastern Ethiopian High Lands with associated low lands*.
- Astatke, K., Yosef, T., & Yonas, M. (2009). *Hydrogeological Mapping of Part of Asela Map Sheet (NB 37-3) South Eastern High Land of Ethiopia*.
- Awan, U. K., & Ismaeel, A. (2014). A new technique to map groundwater recharge in irrigated areas using a SWAT model under changing climate. *Journal of Hydrology*, 519(PB), 1368–1382. <https://doi.org/10.1016/j.jhydrol.2014.08.049>

- Bakker, M., Bartholomeus, R. P., & Ferré, T. P. A. (2013). Preface Groundwater recharge: Processes and quantification. In *Hydrology and Earth System Sciences* (Vol. 17, Issue 7, pp. 2653–2655). <https://doi.org/10.5194/hess-17-2653-2013>
- Banimahd, S. A., Khalili, D., Zand-Parsa, S., & Kamgar-Haghighi, A. A. (2017). Groundwater potential recharge estimation in bare soil using three soil moisture accounting models: field evaluation for a semi-arid foothill region. *Arabian Journal of Geosciences*, 10(10). <https://doi.org/10.1007/s12517-017-3018-9>
- Basalfew, Z., Mathios, A., Meskerem, T., Mekdes, T., Mekonen, B., Mohamed, E., Getachew, B., & Yehualashet, E. (2012). *Geological Map Sheet of Hosaena Area*.
- Berhe, S. M., Desta, B., Nicolett13, M., & Teferra4, M. (1987). Geology, geochronology and geodynamic implications of the Cenozoic magmatic province in W and SE Ethiopia. *Journal of the Geological Society*, 144, 213–226.
- Beven, K. J. (2006). *Rainfall-runoff modelling\_ the primer-John Wiley and Sons (2004)*.
- Billi, P. (2015). Geomorphological Landscapes of Ethiopia. *World Geomorphological Landscapes*, 3–32. [https://doi.org/10.1007/978-94-017-8026-1\\_1](https://doi.org/10.1007/978-94-017-8026-1_1)
- Bridget, R. S., Richard, W. H., & Peter, G. C. (2002). Choosing appropriate techniques for quantifying groundwater recharge. *Hydrogeology Journal*, 10, 18–39. <https://doi.org/10.1007/s10040-0010176-2>
- Busico, G., Ntona, M. M., Carvalho, S. C. P., Patrikaki, O., Voudouris, K., & Kazakis, N. (2021). Simulating Future Groundwater Recharge in Coastal and Inland Catchments. *Water Resources Management*, 35(11), 3617–3632. <https://doi.org/10.1007/s11269-021-02907-2>
- Caritat, O. M. S. and P. De. (1997). *Geochemical Processes, Weathering and Groundwater Recharge in Catchments*. A.A.BALKEMA/ROTTERDAM/BROOKFIELD.
- Cuceloglu, G., Abbaspour, K. C., & Ozturk, I. (2017). Assessing the water-resources potential of Istanbul by using a soil and water assessment tool (SWAT) hydrological model. *Water (Switzerland)*, 9(10). <https://doi.org/10.3390/w9100814>

- Cunderlik, J. M. (2003). Hydrologic model selection for the CFCAS project : Assessment of Water Resources Risk and Vulnerability to Changing Climatic Conditions October 2003 Prepared by Juraj M . Cunderlik University of Western Ontario. In *October* (Issue October).
- Dehghan, R., Pouyan, B., Marjan, N., Molaei, S., Khosravi, H., & Azarnivand, H. (2024). Assessment of groundwater resources potential using Improved Water Quality Index (ImpWQI) and entropy-weighted TOPSIS model. *Sustainable Water Resources Management*, *10*(1). <https://doi.org/10.1007/s40899-023-00988-y>
- Demlie, M. (2015). Assessment and estimation of groundwater recharge for a catchment located in highland tropical climate in central Ethiopia using catchment soil–water balance (SWB) and chloride mass balance (CMB) techniques. *Environmental Earth Sciences*, *74*(2), 1137–1150. <https://doi.org/10.1007/s12665-015-4099-y>
- Gassman, P. W., Reyes, M. R., Green, C. H., & Arnold, J. G. (2007). *The Soil and Water Assessment Tool: Historical Development, Applications, and Future Research Directions*. *50*(4), 1211–1250.
- Gerhat, J. M. (1986). Groundwater Recharge and its Effect on Nitrate Concentration Beneath a manured Field Site in Pennsylvania. *U.S Geological Surveys*. <https://doi.org/https://doi.org/10.1111/j.1745-6584.1986.tb01027.x>
- Gobena, H., Belayneh, M., & Abraham, A. (1997). *Geology of the Dodola Area*.
- Grasso, D. A., Jeannin, P. Y., & Zwahlen, F. (2003). A deterministic approach to the coupled analysis of karst springs' hydrographs and chemographs. *Journal of Hydrology*, *271*(1–4), 65–76. [https://doi.org/10.1016/S0022-1694\(02\)00321-9](https://doi.org/10.1016/S0022-1694(02)00321-9)
- Guzman, J. A., Moriasi, D. N., Gowda, P. H., Steiner, J. L., Starks, P. J., Arnold, J. G., & Srinivasan, R. (2015). A model integration framework for linking SWAT and MODFLOW. *Environmental Modelling and Software*, *73*, 103–116. <https://doi.org/10.1016/j.envsoft.2015.08.011>
- Han, D., Currell, M. J., Cao, G., & Hall, B. (2017). Alterations to groundwater recharge due to anthropogenic landscape change. *Journal of Hydrology*, *554*, 545–557.

<https://doi.org/10.1016/j.jhydrol.2017.09.018>

Healy, R. w. (2017). *Estimating Groundwater Recharge* (Vol. 4, Issue 1).

Jannis, E., Adrien, M., Annette, A., & Peter, H. (2021). Climate change effects on groundwater recharge and temperatures in Swiss alluvial aquifers. *Journal of Hydrology X*, *11*, 100071. <https://doi.org/10.1016/j.hydroa.2020.100071>

Jeffrey, G. A., Peter, M. A., & Gilbert, B. c. (1993). A comprehensive surface-groundwater flow model. *Journal of Hydrology*, *142*, 47–69.

Jinno, K., Tsutsumi, A., Alkaeed, O., Saita, S., & Berndtsson, R. (2009). Effects of land-use change on groundwater recharge model parameters. *Hydrological Sciences Journal*, *54*(2), 300–315. <https://doi.org/10.1623/hysj.54.2.300>

Kebede, S. (2013). Groundwater in Ethiopia: Features, numbers and opportunities. In *Groundwater in Ethiopia: Features, Numbers and Opportunities*. Springer Hydrogeology. <https://doi.org/10.1007/978-3-642-30391-3>

Kiflu, A. and M. H. (2010). *Integrated Hydrogeological Mapping of Dodola Map Sheet (NB 37-7) South Eastern Ethiopian High Lands with associated low lands*.

Kim, N. W., Chung, I. M., Won, Y. S., & Arnold, J. G. (2008). Development and application of the integrated SWAT-MODFLOW model. *Journal of Hydrology*, *356*(1–2), 1–16. <https://doi.org/10.1016/j.jhydrol.2008.02.024>

Larbi, I., Obuobie, E., Verhoef, A., Julich, S., Feger, K. H., Bossa, A. Y., & Macdonald, D. (2020). Water balance components estimation under scenarios of land cover change in the Veve catchment, West Africa. *Hydrological Sciences Journal*, *65*(13), 2196–2209. <https://doi.org/10.1080/02626667.2020.1802467>

Mjemah, I. C., van Camp, M., Martens, K., & Walraevens, K. (2011). Groundwater exploitation and recharge rate estimation of a quaternary sand aquifer in Dar-es-Salaam area, Tanzania. *Environmental Earth Sciences*, *63*(3), 559–569. <https://doi.org/10.1007/s12665-010-0723-z>

Mohr, P.A. and Potter, E. C. (1976). *The Sagatu Ridge Dike Swarm, Ethiopian Rift Margin*.

- Mohr, P. (1983). The Ethiopian flood basalt province. *Continental Flood Basalts*, 63–110. [https://doi.org/10.1007/978-94-015-7805-9\\_3](https://doi.org/10.1007/978-94-015-7805-9_3)
- Moriasi, D. N., Arnold, J. G., Liew, M. W. Van, Bingner, R. L., Harmel, R. D., & Veith, T. L. (2007). *Model Evaluation Guidelines for Systematic Quantification of Accuracy in Watershed Simulations*. 50(3), 885–900.
- Moriasi, D. N., Rossi, C. G., Arnold, J. G., & Tomer, M. D. (2012). Evaluating hydrology of the Soil and Water Assessment Tool (SWAT) with new tile drain equations. *Journal of Soil and Water Conservation*, 67(6), 513–524. <https://doi.org/10.2489/jswc.67.6.513>
- Nasiri, S., Ansari, H., & Ziaei, A. N. (2020). Simulation of water balance equation components using SWAT model in Samalqan Watershed (Iran). *Arabian Journal of Geosciences*, 13(11). <https://doi.org/10.1007/s12517-020-05366-y>
- Neitch, S. L., Arnold, J. G., Kiniry, J. R., & Williams, J. R. (2005). *Soil and Water Assessment Tool Documentation*. Blackland Research Center.
- Neitsch, S. ., Arnold, J. ., Kiniry, J. ., & Williams, J. . (2011). Soil & Water Assessment Tool Theoretical Documentation Version 2009. *Texas Water Resources Institute*, 1–647. <https://doi.org/10.1016/j.scitotenv.2015.11.063>
- Saltelli, A., Tarantola, S., & Chan, K. P. S. (1999). A quantitative model-independent method for global sensitivity analysis of model output. *Technometrics*, 41(1), 39–56. <https://doi.org/10.1080/00401706.1999.10485594>
- Santhi, C., Arnold, J. G., Williams, J. R., Dugas, W. A., Srinivasan, R., & Hauck, and L. M. (2002). *Validation of the SWAT Model on a Large River Basin with Point and Nonpoint Sources*. 37(5), 1169–1188.
- Setegn, S. G., Dargahi, B., Srinivasan, R., & Melesse, A. M. (2010). Modeling of sediment yield from anjeni-gauged watershed, Ethiopia using swat modell. *Journal of the American Water Resources Association*, 46(3), 514–526. <https://doi.org/10.1111/j.1752-1688.2010.00431.x>
- Stephen, A. T. (1999). *Hydrogeology for Water Management*. A.A.Balkema, PO. Box 1675,3000 BR Rotterdam, Netherlands.

- Tilahun, K., & Sima, J. (2013). *Hydrogeological and Hydrochemical Maps of Hosaina Nb 37-2*.
- Trivedi, A., Awasthi, M. K., Gautam, V. K., Pande, C. B., & Din, N. M. (2023). Evaluating the groundwater recharge requirement and restoration in the Kanari river, India, using SWAT model. *Environment, Development and Sustainability*. <https://doi.org/10.1007/s10668-023-03235-8>
- Workineh, H., Daba, B., Mekonen, B., Desalegn, D., & Muluken, Kebede and Mohamed, E. (2014). *Geology, Geochemistry, and Gravity Survey of Asela Area*.
- Workineh, H., Daba, B., Muluken, K., Mekonen, B., & Desalgn, D. (2013). *Geological Map of Asela Map Sheet (NB 37-3)*.
- Wu, K., & Johnston, C. A. (2007). Hydrologic response to climatic variability in a Great Lakes Watershed: A case study with the SWAT model. *Journal of Hydrology*, 337(1–2), 187–199. <https://doi.org/10.1016/j.jhydrol.2007.01.030>
- Zanettin, B., Bellieni, G., and Visentin, E. J. (2006). New radiometric age of volcanic rocks in the central Eritrean plateau (from Asmara to Adi Quala): Considerations on stratigraphy and correlations. *Journal of African Earth Sciences*, 45(2), 156–161. <https://doi.org/10.1016/j.jafrearsci.2006.01.010>

## APPENDIXES

**Appendix 1. Average annual precipitation in millimeters at each meteorological station**

<b>Year</b>	<b>Adaba</b>	<b>Ardayita</b>	<b>Dodola</b>	<b>Hunte</b>	<b>Kofale</b>	<b>Mararo</b>	<b>Annual Average</b>
<b>1998</b>	1050.50	970.53	866.54	1035.30	1215.13	1006.33	1024.04
<b>1999</b>	1016.53	1010.21	1048.25	1006.13	911.17	878.32	978.44
<b>2000</b>	771.43	997.66	889.34	844.46	1028.87	1013.57	924.22
<b>2001</b>	836.20	1024.18	1116.90	685.64	863.84	983.08	918.31
<b>2002</b>	981.34	855.98	967.37	768.98	1009.22	1032.04	935.82
<b>2003</b>	1069.67	944.11	1075.26	913.73	1069.47	1057.74	1021.66
<b>2004</b>	795.24	862.10	1003.63	764.90	997.76	894.23	886.31
<b>2005</b>	1033.47	775.91	1016.53	880.97	1142.76	921.98	961.93
<b>2006</b>	771.20	850.90	886.90	973.80	1013.13	1083.20	929.85
<b>2007</b>	1035.12	846.70	1017.90	846.10	1051.35	1021.21	969.73
<b>2008</b>	927.12	920.30	853.50	915.90	1224.73	1031.40	978.83
<b>2009</b>	1029.90	951.50	849.55	1015.00	1191.30	986.60	1003.96
<b>2010</b>	996.60	990.40	1027.70	986.40	893.30	861.10	959.25
<b>2011</b>	756.30	978.10	871.90	827.90	1008.70	993.70	906.10
<b>2012</b>	819.80	1004.10	1095.00	672.20	846.90	963.80	900.30
<b>2013</b>	962.10	839.20	948.40	753.90	989.43	1011.80	917.47
<b>2014</b>	1048.70	925.60	1054.18	895.81	1048.50	1037.00	1001.63
<b>2015</b>	779.65	845.20	983.95	749.90	978.20	876.70	868.93
<b>2016</b>	1013.21	760.70	996.60	863.70	1120.35	903.90	943.07
<b>2017</b>	1082.10	955.30	865.90	767.80	974.20	1022.00	944.55
<b>2018</b>	881.70	832.70	887.20	750.50	1024.51	768.10	857.45

**Appendix 2. Average annual temperature in degrees Celsius for each meteorological station.**

<b>Year</b>	<b>Adaba</b>	<b>Ardayita</b>	<b>Dodola</b>	<b>Hunte</b>	<b>Kofale</b>	<b>Mararo</b>
<b>1998</b>	15.81	15.50	14.25	15.53	13.29	12.62
<b>1999</b>	15.58	15.48	15.56	14.46	12.98	12.56
<b>2000</b>	15.13	15.68	14.47	15.82	12.57	13.27
<b>2001</b>	14.73	15.40	14.44	16.13	12.83	13.10
<b>2002</b>	14.85	15.22	14.72	16.27	15.74	13.77
<b>2003</b>	14.56	15.78	13.20	15.48	13.31	13.38
<b>2004</b>	14.65	15.70	14.55	15.27	13.17	13.26
<b>2005</b>	15.12	15.85	14.69	15.81	12.37	12.51
<b>2006</b>	14.82	15.54	14.40	15.50	12.13	12.26
<b>2007</b>	15.35	15.95	14.56	15.62	12.11	11.78
<b>2008</b>	14.12	15.53	12.63	15.78	12.02	11.99
<b>2009</b>	14.30	15.36	14.27	15.27	12.44	12.47
<b>2010</b>	15.99	15.41	14.39	13.53	11.97	12.55
<b>2011</b>	15.50	15.20	13.97	15.23	13.03	12.37
<b>2012</b>	15.27	15.18	15.25	14.18	12.73	12.31
<b>2013</b>	14.83	15.37	14.19	15.51	12.32	13.01
<b>2014</b>	14.44	15.10	14.16	15.81	12.58	12.84
<b>2015</b>	14.56	14.92	14.43	15.95	15.43	13.50
<b>2016</b>	14.27	15.47	12.94	15.18	13.05	13.12
<b>2017</b>	14.36	15.39	14.26	15.95	12.91	13.00
<b>2018</b>	15.96	15.93	14.40	16.04	11.99	12.30
<b>Mean</b>	14.96	15.47	14.27	15.49	12.90	12.76

**Appendix 3. Monthly river discharge measurements in mm for the Furuna outlet.**

<b>Year</b>	<b>Jan</b>	<b>Feb</b>	<b>Mar</b>	<b>Apr</b>	<b>May</b>	<b>Jun</b>	<b>Jul</b>	<b>Aug</b>	<b>Sep</b>	<b>Oct</b>	<b>Nov</b>	<b>Dec</b>
<b>2000</b>	0.151	0.128	0.285	0.364	2.338	3.094	5.537	7.667	5.459	3.580	1.662	0.810
<b>2001</b>	0.497	0.086	1.041	1.675	0.812	0.462	2.688	9.243	4.889	3.003	1.503	0.678
<b>2002</b>	1.578	0.052	0.469	2.190	4.083	1.696	4.634	12.247	4.791	3.005	1.484	0.681
<b>2003</b>	0.182	0.168	0.661	0.924	0.216	0.168	1.466	7.187	2.417	2.235	1.359	0.673
<b>2004</b>	0.233	0.040	0.159	0.378	1.666	2.183	5.124	8.236	6.457	2.863	1.409	1.069
<b>2005</b>	0.172	0.064	0.651	0.356	0.410	1.850	5.182	8.947	6.217	4.406	2.681	2.087
<b>2006</b>	0.528	0.124	0.055	0.153	2.036	3.085	7.832	9.213	7.005	3.444	1.686	0.756
<b>2007</b>	0.064	0.038	0.297	0.369	1.093	5.039	8.205	5.243	3.913	2.370	1.139	0.246
<b>2008</b>	1.330	1.312	0.850	0.634	0.244	1.800	6.817	15.090	5.020	2.919	2.393	3.550
<b>2009</b>	0.443	0.111	0.053	2.281	0.519	0.338	4.426	14.980	6.885	3.998	2.127	3.550
<b>2010</b>	1.550	3.620	5.688	2.559	2.554	1.949	4.694	11.040	5.298	2.918	1.498	0.565
<b>2011</b>	0.148	0.126	0.280	0.358	2.297	3.039	5.439	7.531	5.362	3.517	1.633	0.796
<b>2012</b>	0.488	0.084	1.023	1.645	0.798	0.454	2.640	9.080	4.803	2.950	1.476	0.666
<b>2013</b>	1.550	0.051	0.461	2.151	4.011	1.666	4.552	12.030	4.706	2.952	1.458	0.669
<b>2014</b>	0.179	0.165	0.649	0.908	0.212	0.165	1.440	7.060	2.374	2.195	1.335	0.661
<b>2015</b>	0.229	0.039	0.156	0.371	1.637	2.144	5.033	8.090	6.343	2.812	1.384	1.050
<b>2016</b>	0.169	0.063	0.639	0.350	0.403	1.817	5.090	8.789	6.107	4.328	2.634	2.050
<b>2017</b>	0.519	0.122	0.054	0.150	2.000	3.030	7.694	9.050	6.881	3.383	1.656	0.743
<b>2018</b>	0.063	0.037	0.292	0.362	1.074	4.950	8.060	5.150	3.844	2.328	1.119	0.242

**Appendix 4. Monthly river discharge measurements in mm for the Leliso outlet.**

<b>Year</b>	<b>Jan</b>	<b>Feb</b>	<b>Mar</b>	<b>Apr</b>	<b>May</b>	<b>Jun</b>	<b>Jul</b>	<b>Aug</b>	<b>Sep</b>	<b>Oct</b>	<b>Nov</b>	<b>Dec</b>
<b>2000</b>	0.978	0.947	1.003	1.070	1.110	5.127	8.706	13.547	4.523	3.164	1.040	1.000
<b>2001</b>	1.001	2.597	0.968	2.577	1.008	3.467	7.252	11.512	9.728	7.680	8.163	4.088
<b>2002</b>	2.072	0.962	3.073	2.027	1.008	1.665	0.937	11.722	6.142	3.596	2.092	3.334
<b>2003</b>	3.137	7.670	9.185	10.054	0.886	3.045	11.545	16.038	17.724	8.489	2.602	0.932
<b>2004</b>	0.913	2.159	0.888	3.076	0.886	8.485	11.714	16.705	5.765	1.080	1.044	0.993
<b>2005</b>	3.083	0.988	1.054	0.957	6.112	10.697	13.755	14.352	4.635	1.150	1.071	0.992
<b>2006</b>	4.064	9.184	8.271	6.825	3.056	3.415	3.025	17.830	14.394	9.157	4.179	1.031
<b>2007</b>	1.030	0.407	1.008	0.998	1.049	1.044	1.178	5.297	5.219	1.090	1.042	1.074
<b>2008</b>	1.441	0.904	0.827	0.846	1.012	2.990	3.008	11.009	10.012	8.810	6.909	5.001
<b>2009</b>	3.635	2.110	3.005	3.500	4.000	1.304	3.434	3.120	3.130	2.550	3.214	5.882
<b>2010</b>	3.990	9.016	8.120	6.700	3.000	3.353	2.970	17.504	14.131	8.990	4.103	1.012
<b>2011</b>	1.011	0.400	0.990	0.980	1.030	1.025	1.156	5.200	5.124	1.070	1.023	1.054
<b>2012</b>	0.960	0.954	0.959	4.550	3.000	7.304	10.160	11.060	8.551	3.000	1.022	0.994
<b>2013</b>	0.960	0.930	0.985	1.050	1.090	5.033	8.547	13.300	4.440	3.106	1.021	0.982
<b>2014</b>	0.983	2.550	0.950	2.530	0.990	3.404	7.120	11.302	9.550	7.540	8.014	4.013
<b>2015</b>	2.034	0.944	3.017	1.990	0.990	1.635	0.920	11.508	6.030	3.530	2.054	3.273
<b>2016</b>	3.080	7.530	9.017	9.870	0.870	2.989	11.334	15.745	17.400	8.334	2.554	0.915
<b>2017</b>	0.896	2.120	0.872	3.020	0.870	8.330	11.500	16.400	5.660	1.060	1.025	0.975
<b>2018</b>	3.027	0.970	1.035	0.940	6.000	10.502	13.504	14.090	4.550	1.129	1.051	0.974

**Appendix 5. Monthly river discharge measurements in mm for the Wabe outlet.**

<b>Year</b>	<b>Jan</b>	<b>Feb</b>	<b>Mar</b>	<b>Apr</b>	<b>May</b>	<b>Jun</b>	<b>Jul</b>	<b>Aug</b>	<b>Sep</b>	<b>Oct</b>	<b>Nov</b>	<b>Dec</b>
<b>2000</b>	5.094	11.013	30.472	26.010	19.357	37.696	75.391	98.824	58.999	38.714	14.263	9.169
<b>2001</b>	7.600	3.698	12.205	6.948	24.115	31.124	61.067	81.310	62.952	39.784	25.898	12.847
<b>2002</b>	2.027	1.538	5.237	17.707	31.888	46.610	60.996	71.143	50.940	45.846	29.240	14.752
<b>2003</b>	3.393	6.938	21.079	17.299	28.944	36.728	53.049	64.979	57.674	63.828	32.214	18.012
<b>2004</b>	2.608	11.472	24.421	35.444	39.244	47.721	69.574	100.719	70.338	64.714	37.339	18.114
<b>2005</b>	4.126	5.451	15.170	23.432	15.282	34.690	69.278	113.087	56.034	53.996	35.515	25.012
<b>2006</b>	5.654	15.425	12.154	22.475	40.905	60.985	74.851	98.824	69.309	72.477	46.488	25.552
<b>2007</b>	3.148	7.050	10.127	13.764	34.303	70.369	99.842	116.041	73.578	44.511	23.005	15.710
<b>2008</b>	2.600	2.020	9.540	15.270	30.410	37.840	60.000	66.110	50.000	35.000	22.000	5.000
<b>2009</b>	3.050	3.220	11.000	13.000	7.500	35.000	63.130	71.000	42.000	28.000	12.300	8.700
<b>2010</b>	5.000	10.810	29.910	25.530	19.000	37.000	74.000	97.000	57.910	38.000	14.000	9.000
<b>2011</b>	7.460	3.630	11.980	6.820	23.670	30.550	59.940	79.810	61.790	39.050	25.420	12.610
<b>2012</b>	1.990	1.510	5.140	17.380	31.300	45.750	59.870	69.830	50.000	45.000	28.700	14.480
<b>2013</b>	3.330	6.810	20.690	16.980	28.410	36.050	52.070	63.780	56.610	62.650	31.620	17.680
<b>2014</b>	2.560	11.260	23.970	34.790	38.520	46.840	68.290	98.860	69.040	63.520	36.650	17.780
<b>2015</b>	4.050	5.350	14.890	23.000	15.000	34.050	68.000	111.000	55.000	53.000	34.860	24.550
<b>2016</b>	5.550	15.140	11.930	22.060	40.150	59.860	73.470	97.000	68.030	71.140	45.630	25.080
<b>2017</b>	3.090	6.920	9.940	13.510	33.670	69.070	98.000	113.900	72.220	43.690	22.580	15.420
<b>2018</b>	2.980	11.480	9.080	16.640	20.410	39.360	55.990	66.000	49.840	35.790	29.420	14.340

## **RESEARCH FUND ACKNOWLEDGEMENT**

This research thesis was funded by Adama Science and Technology University under the grant number of ASTU/SM-R/971/24, Adama, Ethiopia.